MASTERARBEIT | MASTER'S THESIS

Titel | Title

Investigation of a novel disease-associated GABA transporter 1 variant

verfasst von | submitted by

Marina Lukenic BSc

angestrebter akademischer Grad | in partial fulfilment of the requirements for the degree of

Master of Science (MSc)

Wien | Vienna, 2026

Studienkennzahl lt. Studienblatt | Degree programme code as it appears on the student record sheet:	UA 066 232
Studienrichtung lt. Studienblatt | Degree programme as it appears on the student record sheet:	Masterstudium Neuroscience
Betreut von | Supervisor:	Mag. Thomas Steinkellner PhD

Acknowledgements

First and foremost, I would like to thank Assistant Professor Thomas Steinkellner for giving me the opportunity to contribute to his research and for his constant supervision throughout my project. Through his extensive expertise and feedback, I was encouraged to work independently and was consistently challenged to improve my scientific skills. His trust and continuous guidance were key in helping me gain confidence in my work and develop as a researcher.

Furthermore, I would like to thank my dear colleagues, who welcomed me warmly into the group. Their constant openness to exchanging ideas and unwavering support helped me navigate through my work with ease. I will always look back at my time in the Steinkellner lab with positivity and utter appreciation.

Last but not least, I want to say thank you to Associate Professor Sonja Sucic, who generously provided the eYFP-hGAT1^{WT} plasmid, which played a central role in the initiation and implementation of my project.

Zusammenfassung

Morbus Parkinson (PD) ist eine progressive, neurodegenerative Erkrankung, die primär das motorische System betrifft. Die Ursache der motorischen Symptome ist der selektive Verlust dopaminerger (DA) Neurone in der Substantia nigra *pars compacta*. Die pathologischen Mechanismen jedoch, welche zu dieser selektiven Vulnerabilität führen, sind noch nicht zur Gänze aufgeklärt und Gegenstand aktueller Forschung. Dopaminerge Neuronen sind vielfältig und in der Lage, neben Dopamin, weitere Neurotransmitter freizusetzen. Zum Beispiel konnte gezeigt werden, dass GABA, der bedeutendste inhibitorische Neurotransmitter des zentralen Nervensystems, von dopaminergen Neuronen mitfreigesetzt werden kann. Diese DA/GABA-co-freisetzenden Neurone exprimieren den GABA Transporter 1 (GAT1), welcher notwendig ist, um diese Neurone mit GABA zu versorgen.

Interessanterweise wurde in einem Patienten mit dopaminerger Neurodegeneration und Parkinson-Symptomen eine *de novo* Mutation im GAT1 Gen identifiziert, wo ein Aminosäuretausch von Glycin zu Serin an Position 63 ($GAT1^{G63S}$) stattgefunden hat. Ziel dieser Arbeit war es, die neu identifizierte Variante zu untersuchen, indem ihre Transportfunktion mittels Radioliganden-Aufnahmeassays in HEK293 Zellen analysiert wurde, sowie anschließend virale Vektoren zu generieren, welche die Überexpression von $GAT1^{WT}$ und $GAT1^{G63S}$ für zukünftige *in vivo* Experimente ermöglichen soll. Meine Ergebnisse zeigen, dass die $GAT1^{G63S}$ Mutation zu einem vollständigen Verlust der Transportfunktion führt, jedoch nicht die Lokalisation des Transporters an der Plasmamembran beeinflusst. Nach der Analyse der Funktion und Expression von $GAT1^{G63S}$, wurden Adeno-assoziierte Viren (AAVs) in TSA201 Zellen hergestellt und deren Transduktionseffizienz sowohl *in vitro* wie auch *in vivo* getestet. Insgesamt verdeutlichen meine Ergebnisse, dass die neue GAT1 Variante $GAT1^{G63S}$ an der Plasmamembran exprimiert wird, jedoch transportdefizient ist. Die AAVs werden in weiteren *in vivo* Studien eingesetzt um die Untersuchung von GAT1 in dopaminergen Neuronen und deren Zusammenhang mit der selektiven Vulnerabilität in PD, zu testen.

Abstract

Parkinson's disease (PD) is a progressive neurodegenerative motor disorder. The cause of motor symptoms is the specific degeneration of dopaminergic (DA) neurons in the substantia nigra *pars compacta*. However, pathological mechanisms accounting for this selective vulnerability are still not fully understood and subject of ongoing research. DA neurons are diverse and many have the ability to co-release another small molecule neurotransmitter besides DA. For instance, GABA, the major inhibitory neurotransmitter within the central nervous system, has been found to be co-released from DA neurons. The DA/GABA co-releasing neurons express GABA transporter 1 (GAT1) which seems to be necessary to supply these DA neurons with GABA.

Interestingly, a *de novo* mutation in GAT1, namely the amino acid substitution Gly63Ser ($GAT1^{G63S}$), was found in an individual who presented with DA neurodegeneration and parkinsonian symptoms. The aim of my thesis was to explore this new variant by means of investigating its transporter function using radioligand uptake assays in HEK293 cells and to thereafter establish a viral vector that allows for the overexpression of $GAT1^{WT}$ and $GAT1^{G63S}$ for future *in vivo* investigations. My results show that the $GAT1^{G63S}$ mutation caused abolishment of transport activity but did not compromise trafficking to the plasma membrane. After assessing expression and function of $GAT1^{G63S}$, adeno-associated vectors (AAVs) were generated in TSA201 cells and transduction efficiency was confirmed *in vitro* and *in vivo*. Overall, my findings highlight that the newly identified GAT1 variant $GAT1^{G63S}$ is expressed at the plasma membrane but transport-deficient. The AAVs I have prepared will aide further in vivo studies addressing the role of the GAT1 in DA neurons and their relation to selective vulnerability in PD.

Table of Contents

List of Illustrations

List of Abbreviations

AADC	Aromatic L-amino acid decarboxylase
AAV	Adeno-associated virus
ALDH	Aldehyde dehydrogenase
ASYN	α-synuclein
ATP	adenosine triphosphate
BBB	Blood brain barrier
Cl^-	chloride ion
CNS	Central nervous system
cpm	counts per minute
D1 – D5	Dopamine receptors 1 – 5
DA	Dopaminergic
DAT	Dopamine transporter
DMEM	Dulbecco's Modified Eagle Medium
FBS	Fetal bovine serum
GABA	Gamma-aminobutyric acid
$GABA_AR$	GABA receptor type A
$GABA_BR$	GABA receptor type B
GAD	Glutamate decarboxylase
GAT1	Gamma-aminobutyric acid transporter 1
GIRK nels	G-protein activated inwardly rectifying K^+-chan-
HEK cells	Human embryonic kidney cells
hGAT1	human GABA Transporter 1

K^+	potassium ion
KHB	Krebs-HEPES buffer
L-DOPA	L-3,4-dihydroxyphenylalanine
LB	Lewy Body
1-methyl-4-phenylpyridinium	MPP+
1-methyl-4-phenyl-1,2,3,6-tetrahydripyridine	MPTP
MAO-B	Monoamine oxidase B
MSN	Medium spiny neuron
mtDNA	mitochondrial DNA
Na^+	sodium ion
o/n	overnight
OXPHOS	Oxidative phosphorylation
P/S	Penicillin-Streptomycin
PBS	Phosphate-buffered saline
PCR	Polymerase Chain Reaction
PD	Parkinson’s Disease
PDL	Poly-D-lysine
PINK1	PTEN-induced kinase 1
ROS	Reactive oxygen species
RT	Room temperature
SLC6	Solute carrier 6
SNc	Substantia nigra pars compacta
TH	tyrosine hydroxylase
TMD	Transmembrane domain

V	Volt
VGAT	vesicular GABA transporter
VGLUT2	vesicular glutamate transporter 2
VMAT2	vesicular monoamine transporter 2
VTA	Ventral tegmental area
WT	Wildtype

1 Introduction

1.1 Parkinson's Disease

Parkinson's disease (PD) is a progressive, neurodegenerative movement disorder, with currently no available curative treatment (Armstrong and Okun, 2020). Approximately 1% of the world's population above 60, which would roughly amount to 10 million people, are affected by PD (Tysnes and Storstein, 2017), with a steadily advancing prevalence with age, with men being more prone to the disease than women (Pringsheim *et al.*, 2014). Most importantly, patients' overall quality of life and mental health suffers tremendously (Zhao *et al.*, 2021), given that diagnosis of certain (non-motor) symptoms is still challenging (Tolosa *et al.*, 2021). Additionally, even though constant progress for future disease-modifying treatments is being made, current therapies are still too short-lived (Poewe *et al.*, 2020).

1.1.1 Neuropathological hallmarks and symptoms

1.1.1.1 Dopaminergic neurodegeneration

First described by James Parkinson in his work "An Essay on the Shaking Palsy" in 1817, the major motor symptoms of the disease were identified as tremor, rigidity and bradykinesia (Parkinson, 1817). These cardinal motor symptoms are linked to the selective loss of dopaminergic (DA) neurons in the substantia nigra pars compacta (SNc) (Surmeier, 2018), which is part of the basal ganglia, a group of subcortical nuclei, central to motor control. The DA neurons projecting from the SNc to the striatum are modulating the so-called direct (activating) and indirect (inhibiting) pathways through medium spiny neurons (MSNs), which in turn connect several brain structures, involving the cortex and thalamus. The interplay of these areas, under physiological conditions, lead to voluntary movements as well as fine motor control. These functions are lost in PD due to DA neurodegeneration, where the imbalance between both pathways leads to an overactivation of the inhibiting signals, thus

impairing coordinated motor function (**Figure 1**) (Gerfen and Surmeier, 2011; Calabresi *et al.*, 2014).

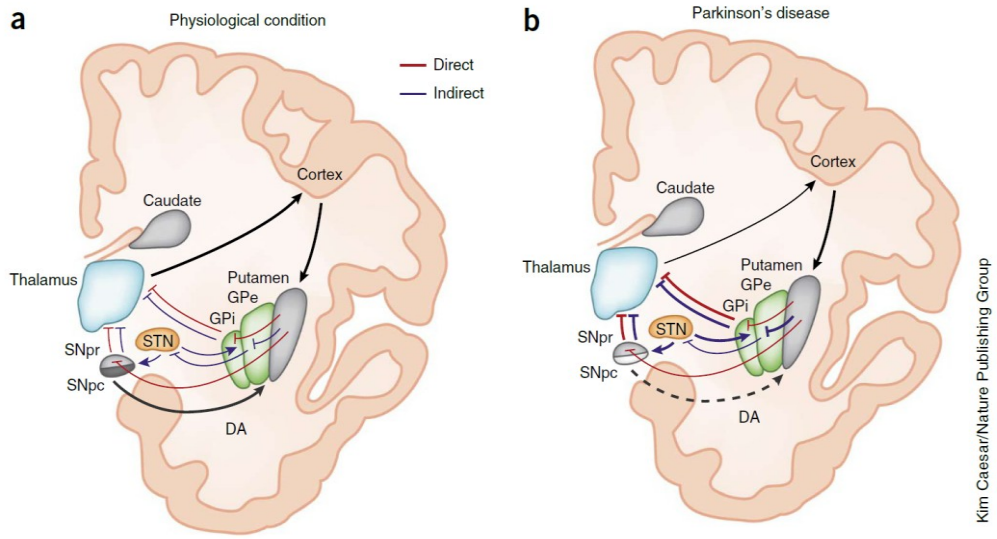

Figure 1 Depiction of direct and indirect pathways in (A) physiological condition and (B) Parkinson's Disease. *Reproduced from Calabresi, P. et al. (Nat. Neurosci., 2014) with permission from Springer Nature. License number: 6198900113667.*

Specifically, the severity of motor dysfunction was found to be associated with the degeneration of DA projections within the striatum in early-stage PD, which progresses to DA soma loss in PD patients with severe motor impairments in later stages of the disease (Furukawa *et al.*, 2022). Additionally, there are several non-motor symptoms which burden patients even years before the first motor manifestations and accompany them throughout the disease progression. These include depression and anxiety, as well as constipation, sleep disturbances and dementia, among others (Schapira, Chaudhuri and Jenner, 2017). There are implications that those symptoms could be emerging due to the damage of the peripheral, autonomic nervous system (Gelpi *et al.*, 2014) and its further investigation could be used as a biomarker for pre-motor or early stage PD patients (Cersosimo and Benarroch, 2012).

There is no disease-modifying therapy available for PD, but rather symptom-alleviating treatment options for patients. Especially in regard to the motor symptoms, several pharmacological interventions were designed to target the DA system in

order to treat the deficiency in dopamine levels (Armstrong and Okun, 2020). In this case, the gold standard treatment comprises the use of L-3,4-dihydroxyphenylalanine (L-DOPA), a dopamine precursor, which was first tested in 1961 in male PD patients by Hornykiewicz and Birkmayer, who were able to report drastic improvement of motor function in PD patients (Birkmayer and Hornykiewicz 1961). Contrary to dopamine, L-DOPA can cross the blood brain barrier (BBB) after which it is converted into dopamine by aromatic L-amino acid decarboxylase (AADC). In order for L-DOPA to not be metabolized into dopamine prematurely, AADC-inhibitors, (carbidopa or benserazide), which cannot cross the BBB, are co-administered to block peripheral AADC activity (Riederer *et al.*, 2025). The addition of AADC-inhibitors greatly improved patients' L-DOPA-related side effects like nausea, however, the continuous treatment with the drug emerged to trigger additional motor complications. The appearance of L-DOPA-induced dyskinesias and so-called *off* periods, where patients stop responding to the treatment and start to experience disabling motor dysfunctions, have especially been correlated to high doses of L-DOPA, among other factors (Warren Olanow *et al.*, 2013), making it harder for patients to navigate the disease. Although L-DOPA has proven to be an effective drug against the cardinal motor symptoms, it does not prevent nor modify PD and its progression in neurodegeneration, showcasing the importance of investigating not only symptom-facilitating, but also disease-modifying approaches (Olanow and Stocchi, 2018; Bandopadhyay *et al.*, 2022).

1.1.1.2 α-synuclein

Besides DA neuron loss, another crucial PD hallmark involves α-synuclein (ASYN), a 140 amino acid containing protein, which is mainly found in presynaptic terminals of neurons, among other non-neuronal cell types, where it is believed to be involved in synaptic function and is able to interact with the lipid membrane (Vekrellis, Rideout and Stefanis, 2004). Insoluble ASYN is a major constituent of intraneuronal, proteinaceous inclusions, so-called Lewy Bodies (LBs) and Lewy Neurites, which can compromise membranes including organelles (Spillantini *et al.*, 1998; Shahmoradian *et al.*, 2019). Pathological misfolding of ASYN involves the generation of insoluble oligomers, which then aggregate into amyloid fibrils and lastly give

rise to LBs (Burré, Sharma and Südhof, 2018). The formation of LBs through fibrillated ASYN and the accumulation of such, were found to be associated with synaptic dysfunction, disrupted neuronal homeostasis and subsequent cell death (Volpicelli-Daley *et al.*, 2011; Mahul-Mellier *et al.*, 2020), highlighting alpha synuclein's integral part to PD pathology.

Through post-mortem research, Braak *et al.* created a neuropathological staging scheme, that describes the progressive emergence of ASYN-positive LBs within different brain areas. The so-called Braak stages are divided into 6 gradually evolving stages, with stages 1 and 2 showing aggregates in the brainstem, which then propagate to the midbrain including the SNc in stage 3 and finally extend throughout cortical areas in stages 4 – 6 (Braak *et al.*, 2003). The different stages can also be related to PD symptom progression, with non-motor symptoms starting in early Braak stages of LB accumulations within the brain and the motor and cognitive manifestations getting worse as the aggregates advance up until the last Braak stage (**Figure 2**) (Koeglsperger *et al.*, 2023). This mechanism of self-aggregation and spreading of ASYN reminds of a "prion-like"-behavior, where misfolded proteins interact with endogenous, native proteins to nucleate their folding into a pathological conformation (Vascellari and Manzin, 2021). Indeed, it has been shown in both *in vitro* as well as *in vivo* studies, that ASYN was able to propagate from cell to cell with subsequent inclusion formation and that the inoculation of pathological ASYN fibrils into transgenic mice lead to the progressive spreading of abnormal protein within the brain and neurodegeneration (Desplats *et al.*, 2009; Luk *et al.*, 2012).

Moreover, ASYN and LB aggregates have not only been found in the central nervous system (CNS), but also in the peripheral autonomic nervous system as well as in multiple organs, such as the gastrointestinal tract, according to post-mortem investigations of PD and REM sleep behavior disorder patients (Beach *et al.*, 2010; Gelpi *et al.*, 2014; Sprenger *et al.*, 2015), with the latter being a known non-motor symptom of PD (Schapira, Chaudhuri and Jenner, 2017). It was even suggested by *Braak et al.*, that the enteric nervous system could be the gateway for the spreading of PD pathology from the periphery into the CNS by their direct connection through the vagal nerve (Braak *et al.*, 2004), which would go along with the findings of ASYN being localized within those sites (Beach *et al.*, 2010; Gelpi *et al.*, 2014).

Nevertheless, these histological findings of LBs outside the CNS could be used as markers for prodromal and early-stage PD in future patient-investigations (Cersosimo and Benarroch, 2012).

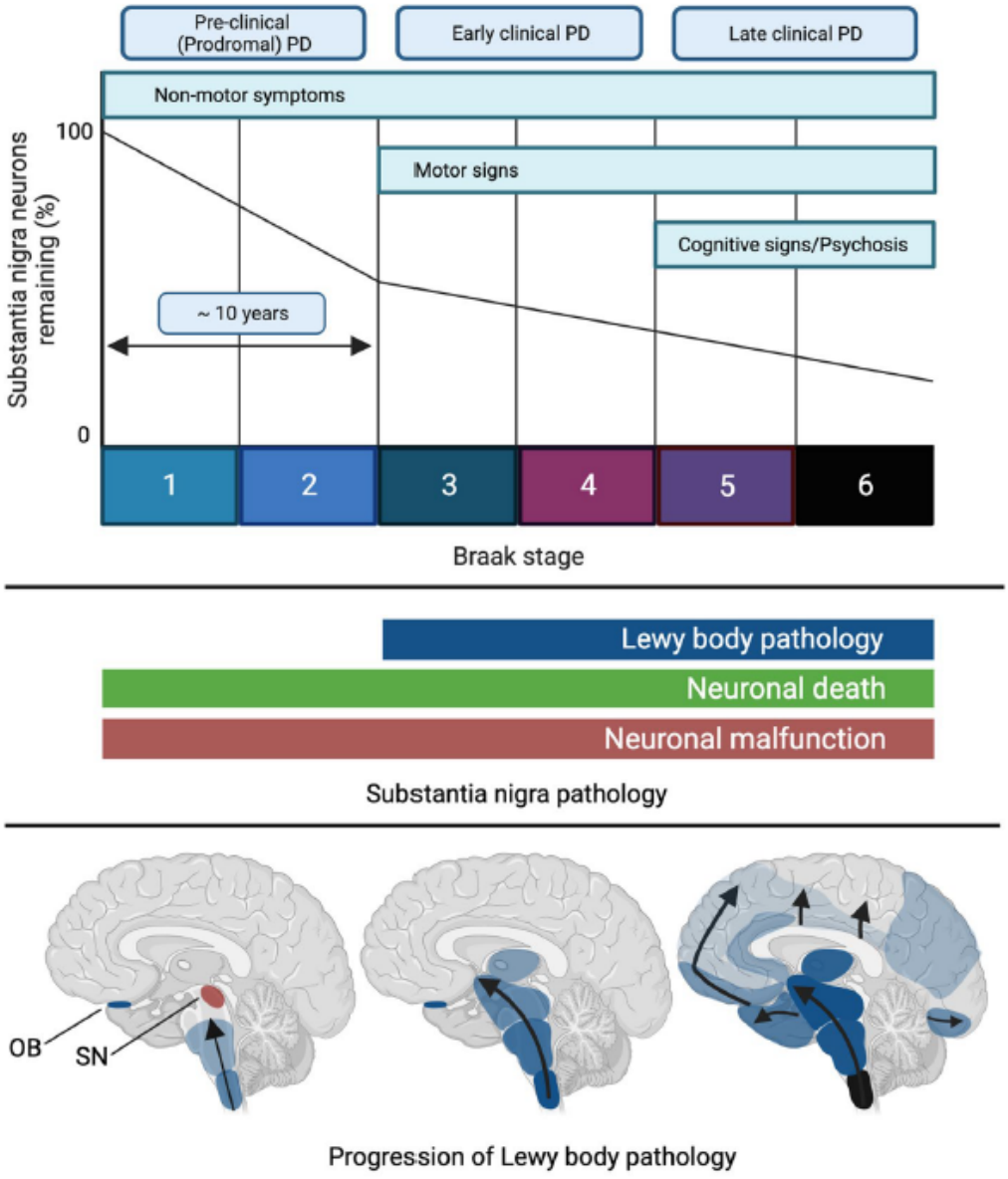

Figure 2 Progression of Lewy Body Pathology in PD in association with DA neuro-degeneration. *In accordance with Braak's staging, the progression from prodromal to late clinical PD is depicted, showing the onset of non-motor and motor symptoms. Reproduced from Koeglsperger, T. et al. (Mol. Neurodegeneration, 2023) under CC BY 4.0 (http://creativecommons.org/licenses/by/4.0/).*

1.1.1.3 Mitochondrial dysfunction

Mitochondria are highly dynamic and self-regulating organelles, whose main functions include the production of energy in form of adenosine triphosphate (ATP) through the process of oxidative phosphorylation (OXPHOS), the regulation of programmed cell death (apoptosis) and the maintenance of calcium homeostasis. Through having their own mitochondrial DNA (mtDNA) and ribosomes, they are able to synthesize a small subset of their own proteins, which mainly serve the complexes of the electron transport chain involved in energy production. However, the remaining proteins needed for the preservation of their structure and function are imported into the different mitochondrial compartments through the interplay of several translocases (Kutik *et al.*, 2007; Protasoni and Zeviani, 2021b). Additionally, these organelles possess over their own quality control mechanisms, where damaged mitochondria are sensed and removed via mitophagy, a mitochondria-specialized autophagy pathway. Worth mentioning in this case is PINK1 (PTEN-induced kinase 1) -Parkin-mediated mitophagy, with both proteins having implications within PD when dysfunctional (Pickles, Vigié and Youle, 2018). PINK1, a mitochondria-localized kinase, is stabilized on the damaged, outer membrane in order to be able to recruit Parkin, a cytosolic, E3-ubiquitin-ligase, by phosphorylating ubiquitin and thereafter Parkin itself, to activate it. Simultaneously, PINK1 recruits mitophagy receptors, independent of Parkin, to initiate the mitophagic process. Parkin then commences its ligase activity by ubiquitinating different target proteins on the mitochondrial membrane, which then finally leads to the degradation of the impaired mitochondria (Narendra *et al.*, 2010; Shiba-Fukushima *et al.*, 2012; Kane *et al.*, 2014; Lazarou *et al.*, 2015; Dunkerley *et al.*, 2022). Certainly, dysfunctional PINK1 and Parkin signaling was found to lead to a disruption of mitophagy, thus leading to the accumulation of senescent mitochondria and impairments within neurons in different PD models associated with PINK1 and Parkin knock-outs and mutant variants (Quinn *et al.*, 2020).

Mitochondria and PD are especially linked through the impairment of the bioenergetic metabolism, including the respiratory chain and OXPHOS. In a gene expression analysis of PD DA neurons, OXPHOS as well as Krebs cycle genes were found to be highly dysregulated (Elstner *et al.*, 2011). Correspondingly, in a study where

brain energetics were investigated, it was found that ATP levels were decreased in PD patient brains (Rango, Bonifati and Bresolin, 2006). Regarding respiratory chain deficiencies, a high number of mtDNA deletions have been detected in SN neurons of PD individuals (Bender *et al.*, 2006), which, as previously mentioned, mainly encode genes from the respiratory chain (Protasoni and Zeviani, 2021a). Especially complex I seems to be the most vulnerable when it comes to its connection in PD: for example, mitochondria that were extracted from PD patient brains show functionally impaired as well as damaged complex I subunits through oxidative stress (Keeney *et al.*, 2006). Reactive oxygen species (ROS) production is, concerning the function of the complexes within the respiratory chain and subsequent OXPHOS, a physiological byproduct, which is contained and controlled through certain mitochondrial enzymes. However, when mitochondria and their antioxidant system dysfunctions, or complexes within the respiratory chain are disordered, ROS levels increase to a damaging extent, where certain biomolecules, including proteins, lipids and (mt)DNA get harmed, which could ultimately lead to the induction of mutations and cell death (Koopman *et al.*, 2012). Lastly, even PINK1 mutations and ASYN accumulations were found to impair complex I function within neurons and PD brains, respectively, which lead to decreased ATP production, impaired synaptic function and possibly heightened ROS production (Devi *et al.*, 2008; Morais *et al.*, 2009).

1.1.1.4 Neuroinflammation

Inflammation is a defense mechanism mediated by the immune system due to the disturbance to or damage of normal cell and tissue function. Within the CNS, inflammatory processes are mainly controlled through microglia, known as the first line of defense in the CNS, which are highly reactive cells and constantly surveille neuronal tissue for aberrant changes. Usually, moderate activation of microglia through pro-inflammatory mediators like cytokines and chemokines help with the rebalancing of overall cellular homeostasis, however, in the case of a dysregulated activation, these inflammatory mechanisms can lead to the opposite effect and induce permanent tissue damage, ergo neurodegeneration, as well as interfere with normal

neuronal and synaptic function (Sochocka, Satler Diniz and Leszek, 2017; Gelders, Baekelandt and Van der Perren, 2018).

Evidence for the presence of neuroinflammation within PD has been shown through several studies. For example, an investigation of PD patient serum for neuroinflammatory markers, has shown significantly elevated levels of several cytokines, such as TNFα and INF-γ (Brodacki *et al.*, 2008). Moreover, in post-mortem brains of individuals with PD, the chemokine receptor CXCR4 and its ligand CXCL12 were highly expressed in the striatum and SN, which was accompanied by an increased number of activated microglia (Shimoji *et al.*, 2009). Another post-mortem study of PD patient midbrains revealed through single-cell sequencing, that there was an increase in pro-inflammatory microglia within the SN, which presented with gene dysregulations in regard to cytokine signaling and reactivity to misfolded proteins. Additionally, besides microglia, other glial cells, such as astrocytes and oligodendrocytes, have been identified as either being overly activated or decreased in cell number, respectively (Smajic *et al.*, 2022). The involvement of ROS, specifically nitric oxide, in combination with pro-inflammatory signaling, has been studied *in vitro*. In one study it has been shown that the presence of pro-inflammatory cytokines leads to the upregulation of receptors which drove the induction of nitric oxide production and in turn, nitric oxide then increased the production of further pro-inflammatory cytokines. Through further investigation of post-mortem brains of PD subjects, the presence of the before-mentioned cytokines, as well as the ROS-inducing receptors found *in vitro*, could be verified (Hunot *et al.*, 1999). Finally, fibrillated ASYN has been shown to activate STING, a distinct microglia-mediated neuroinflammatory pathway, in a PD model, which resulted in an overactivation of pro-inflammatory microglia, genotoxicity and subsequent neurodegeneration. Additionally, increased levels of STING proteins have been found in the SNc of PD patients (Hinkle *et al.*, 2022).

1.1.2 Etiology and risk factors

PD is the second most common neurodegenerative disease (Poewe *et al.*, 2017) and simultaneously the fastest growing neurological disorder, where estimated numbers predict that around 14 million people will be affected by 2040 (Dorsey and Bloem, 2018). The exact etiology of PD is still unclear, since most cases have a

sporadic origin, which is also known as idiopathic PD. However, around 10% of PD individuals have the familial form, which indicates a genetic background of causal mutations. Nevertheless, PD is a multifactorial disease, meaning that its etiology is not only determined by one, but rather by the interplay of several different factors, including genetic and environmental influences (Klein and Westenberger, 2012).

The identifying names for the different genetic mutations refer to the region on the chromosome were the mutation is present (*PARK* loci), which encode for several PD-related proteins like ASYN, mitophagy-related players and more (Klein and Westenberger, 2012). For example, the first causative mutation that was discovered was a mutation of the gene encoding for ASYN, SNCA (also known as PARK1 gene). It was reported, that independent families from different countries carried the amino acid substitution $ASYN^{A53T}$, which was found to cause early-onset PD and was characterized to have an autosomal-dominant inheritance (Polymeropoulos *et al.*, 1997). The most frequent familial forms of PD have mutations in *LRRK2* (autosomal recessive), which encodes for the leucine-rich repeat kinase 2. Post-mortem autopsies showed DA degeneration in the SN as well as LB pathology in individuals of different families (Zimprich *et al.*, 2004). Other mutations include *PARK2* and *PARK6*, which are situated in genes that encode for the mitophagy-related proteins Parkin and PINK1, respectively and were found in families of different ethnicities. In comparison to the other *PARK* mutations, these two are autosomal-recessively inherited and lead to early-onset PD (Kitada *et al.*, 1998; Valente *et al.*, 2001).

Though genetic background plays a crucial role in the onset of familial PD, it still composes only the minority of cases when it comes to the known causes of disease outbreak. Therefore, it is hypothesized that PD etiology is multifactorially influenced. In a case-control study, where patients and control individuals were examined over several years concerning certain environmental factors, exposure to pesticides and herbicides, but also family history of PD and previous depression were associated to a higher risk of PD development (Sanyal *et al.*, 2010). Interestingly, the link to pesticides was made through the herbicide paraquat and its structural similarity to a toxic metabolite of 1-methyl-4-phenyl-1,2,3,6-tetrahydripyridine (MPTP), namely 1-methyl-4-phenylpyridinium (MPP+), which was first discovered in a synthetic drug capable of evoking drug-induced parkinsonism. MPTP is able to cross the BBB and

is then converted into the neurotoxin MPP+ in the CNS, where it was shown to be selectively taken up by DA neurons and thereafter inhibits the mitochondrial complex I, which in turn leads to ROS production and subsequent neurodegeneration (Langston, 2017). Many more pesticides, industrial toxins and air pollutants have been identified to increase the risk of PD (Brolin *et al.*, 2025). On the other hand, factors like physical activity for overall health and, oddly, caffeine intake and smoking, are negatively correlated with PD development (Chen *et al.*, 2021).

1.2 Dopamine neurons

CNS dopamine neurons are mainly located in a brain area called the midbrain, where anatomically distinct cell groups make up the DA system, which are known as the ventral tegmental area (VTA), SNc and the retrorubral field. Different pathways, like the mesocorticolimbic and the nigrostriatal tracts, regulate functions like reward-associated as well as habit learning behaviors and locomotor control, respectively, by connecting several brain areas like the prefrontal cortex or the striatum (Bodea and Blaess, 2015; Huang, 2015). However, disturbances in the DA systems and dopamine signaling can lead to addiction-associated and psychiatric disorders, but also motor diseases like PD (Klein *et al.*, 2019).

1.2.1 General function and signaling

Midbrain DA neurons are identified through the presence of tyrosine hydroxylase (TH), the rate-limiting enzyme in catecholamine biosynthesis, which includes dopamine. Firstly, TH converts the amino acid tyrosine into L-DOPA, which is then decarboxylated into dopamine through AADC (Tekin *et al.*, 2014). Once dopamine is produced, it is stored in synaptic vesicles through which the neurotransmitter is subsequently released into the extracellular space upon an action potential-induced signal. The vesicular packaging process is mediated through the vesicular monoamine transporter 2 (VMAT2), which is located within the synaptic vesicle membrane. VMAT2 uses the electrochemical gradient established through a vacuolar ATPase, that pumps protons into the vesicles to in turn being utilized for an exchange of two protons for one dopamine molecule (Eiden and Schäfer, 2004; Ye *et al.*, 2025). The

acidic environment inside the presynaptic vesicles, created through the presence of protons, is crucial for stabilizing dopamine during its storage due to its potential to autoxidize within neutral pH (Umek *et al.*, 2018).

Extracellular dopamine is usually recycled by the reuptake through the dopamine transporter (DAT). DAT belongs to the solute carrier 6 (SLC6) family, which are sodium-chloride (Na^+-Cl^-)-symporters that use the electrochemical potential difference of Na^+ as an energy source to co-transport substrates, for example dopamine, along the Na^+ gradient into the neuronal cell, which is maintained by the Na^+-K^+ (potassium)-ATPase (Kristensen *et al.*, 2011). After DAT-mediated reuptake of dopamine into the cytosol, DA is either loaded into synaptic vesicles through VMAT2 again as described earlier, or degraded by different enzymes into metabolites, e.g. monoamine oxidase A or B (MAO-A/B). Through MAOs, dopamine is converted into the highly reactive DOPAL, which is further metabolized into DOPAC by aldehyde dehydrogenase (ALDH) and lastly turned into homovanillic acid by catechol-O-methyltransferase (Meiser, Weindl and Hiller, 2013).

DA neurons signal through different firing patterns, which are known as phasic and tonic firing. Both firing types are differentially modulated, leading to either fast and burst-like release of dopamine which is believed to be rather spatially restricted to the DA synapse and intercepted by rapid reuptake or slower and more diffuse release, that is described as pacemaker-like firing (Hyland *et al.*, 2002; Floresco *et al.*, 2003). Additionally, DA neurons are known to signal in a neuromodulatory way called volume transmission, where dopamine release is not necessarily restricted to assigned synaptic contacts but rather discharged through so called varicosities (“en passent”-synapses) found along the nerve fiber, which would lead to neurotransmitter diffusion across the extracellular space, reaching several, neighboring neurons and their receptors (Özçete, Banerjee and Kaeser, 2024). Once dopamine reaches its receptors, different signals are integrated, which depend on the activated receptor type. The five known dopamine receptors (D1 – 5) are so-called G-protein coupled receptors: while D1 and D5 are coupled to activating G-proteins (G_s), D2, D3 and D4 are bound to inhibiting G-proteins (G_i) (Beaulieu and Gainetdinov, 2011). As an example, with focus on the dopamine-modulated locomotion circuitry within the basal ganglia, DA neurons innervate the striatum, where they regulate motor activity

through either D1 or D2 receptors located on MSNs. Under physiological conditions, the direct pathway, mediated through D1, would lead to the disinhibition of excitatory neurons in the thalamus, which are now able to signal to the cortex and activate voluntary movement, whereas activation of the indirect, ergo D2 pathway, would lead to the opposite effect, which induces a decrease in locomotion. Furthermore, the DA modulatory effect vanishes in the case of PD, where an imbalance of the two pathways lead to an overactivation of D2 and therefore overinhibition of movement initiation (**Figure 1**) (Calabresi *et al.*, 2014).

1.2.2 Subtypes and vulnerability

Dopamine neurons have been found to be a heterogeneous population, presenting with not only cell-specific markers like TH or VMAT2. Differential gene expression profiles showcase for example co-existence of vesicular glutamate transporter 2 (VGLUT2), usually found in excitatory or vesicular gamma-aminobutyric acid (GABA) transporter (VGAT), being a feature of inhibitory neurons, besides other markers (Poulin *et al.*, 2014; Conrad *et al.*, 2024). Likewise, the presence of GABA transporter 1 (GAT1) in DA SNc and VTA neurons has been confirmed (Srinivasan *et al.*, 2025). Additionally, DA subpopulations have been found to differ in their projection targets, innervating parts of distinct brain regions (Poulin *et al.*, 2018). Another feature attributed to DA neuron heterogeneity is their implication in disease and selective vulnerability. Accordingly, SNc DA neurons progressively degenerate in PD throughout different stages of disease advancement, with certain neurons even persisting into later PD stages. Interestingly, DA neurons within the VTA are largely spared and resistant in comparison to SNc cells (Surmeier, Obeso and Halliday, 2017). One example of such a subtype that seemingly increases DA neuronal vulnerability in the SNc has been shown to be ALDH1A1-positive cells, which were significantly reduced in a PD model in comparison to neurons which lack the marker for ALDH1A1 (Poulin *et al.*, 2014). Indeed, a subset of ALDH1A1 DA neurons have been found to be enriched in degenerating pathways within PD. These neurons are also co-expressing Sox6, a transcription factor which is mostly found within cells of the ventral part of the SNc and together are implied to be prominently involved in the selective vulnerability of DA neurons within PD (Luppi *et al.*, 2021).

Even further Sox6 subtypes have been shown to be susceptible to degeneration (Kamath *et al.*, 2022) and are involved in early-onset motor deficits found within a PD model (Fushiki *et al.*, 2024). On the other hand, more resilient DA neurons have been found to be located in the dorsal SNc, expressing markers like Calb1 (Kamath *et al.*, 2022), but also VGLUT2, being additionally highly expressed in the VTA (Poulin *et al.*, 2020). Regarding the role of VGLUT2 in PD, it has been shown that its deletion lead to DA neurons being more sensitive to PD-related neurotoxins (Steinkellner *et al.*, 2018) and that PD individuals presented with a significant increase in VGLUT2 expression within the remaining SNc DA neurons (Steinkellner *et al.*, 2022). Further DA subtypes like VGAT-positive cells for example have not directly been connected to vulnerability nor resilience, even though they have been genetically clustered together with the resilient Calb1-positive cells, which may point this subtype into a certain direction (Poulin *et al.*, 2014).

1.2.3 Neurotransmitter co-release

Dale's principle says that one neuron solely releases one type of neurotransmitter from all of their synapses. However, this theory has been refuted several times to date, especially in the context of DA midbrain neurons co-releasing additional neurotransmitters (Sulzer and Rayport, 2000). As mentioned, midbrain DA neurons have been shown to co-express markers like VGLUT2 and VGAT (Poulin *et al.*, 2020; Conrad *et al.*, 2024) with their function primarily being the packaging of glutamate and GABA, respectively, into synaptic vesicles which is a crucial step for neurotransmitter release in general (Omote and Moriyama, 2025).

Co-release is overall defined as the discharge of different neurotransmitters coming from the same vesicle, while co-transmission would implicate that the released vesicles carried one or the other neurotransmitter (Vaaga, Borisovska and Westbrook, 2014). An evident example for co-release within midbrain DA neurons includes GABA and its non-canonical vesicle packaging. It was shown that VGAT was not necessary for GABA release through DA neurons, but rather the transport function of VMAT2 (Tritsch, Ding and Sabatini, 2012). Through electron microscopy, it has been validated that GABA co-localized with VMAT2-positive synaptic vesicles in the rodent striatum (Stensrud, Purchades and Gundersen, 2014). Another

neurotransmitter implicated in co-release is glutamate through VGLUT2, which was found to be co-located on vesicles expressing VMAT2 and facilitating dopamine storage through glutamate co-transport (Hnasko *et al.*, 2010). Additionally, glutamate co-release from SNc DA neurons has been shown to be involved in regulation of striatal-cell activity (Cai and Ford, 2018) as well as in directing development and neuronal survival of DA neurons (Fortin *et al.*, 2012). Considering the given facts, glutamate co-release and the role of VGLUT2 in disease has been supported by detecting VGLUT2 in still existing midbrain DA neurons of post-mortem PD individuals, which would indicate a neuroprotective function through the co-availability of glutamate (Steinkellner *et al.*, 2022). Nevertheless, while glutamate co-release showcases an indicatory progression in PD, the position of GABA-corelease herein is rather underexplored (Barcomb and Ford, 2023).

1.3 GABA Transporter 1

GABA is the major inhibitory neurotransmitter within the central nervous system, regulating the balance of neuronal network inputs and contributes to several physiological functions (Zhang *et al.*, 2024). In order for GABA to be able to work as precisely as possible, the right termination of signaling is crucial. In that case, GAT1 plays a central role in the neurotransmitters reuptake and is widely expressed throughout the CNS (Scimemi, 2014), including the SNc, with implications in GABA co-release in DA neurons (Tritsch *et al.*, 2014; Srinivasan *et al.*, 2025).

1.3.1 General GABA signaling and function

Classical GABA biosynthesis relies heavily on the presence of glutamate within the cell, which is constantly being produced through different pathways within GABAergic neurons, involving the mitochondrial TCA cycle (Bak, Schousboe and Waagepetersen, 2006). Subsequently, glutamate is converted into GABA through glutamate decarboxylase (GAD), with two GAD subtypes being present in GABAergic neurons, namely GAD67 (GAD1) and GAD65 (GAD2), with the latter being directly associated with fast decarboxylation of glutamate into GABA through its imminent localization to synaptic vesicles (Roth and Draguhn, 2012). Once GABA is

produced, it is directly translocated into synaptic vesicles through VGAT (Juge *et al.*, 2009). This process is driven via the electrochemical proton gradient established by a vacuolar ATPase, which pumps protons into the vesicles. Another player which is secondarily responsible for keeping the electrochemical gradient going, is a chloride channel, which exchanges one proton for 2 chloride ions, leading to the stimulation of the ATPase to increase the proton concentration (Omote and Moriyama, 2025).

Once GABA is released into the extracellular space, it is now free to act on the post- and/or presynaptic neuron, where different types of receptors are located, namely $GABA_A$Rs and $GABA_B$Rs (GABA receptor type A and B). $GABA_A$Rs are known as pentameric, ionotropic receptors, meaning that upon GABA binding, they are acting fast within a few milliseconds. This leads to the opening of the ligand-gated anion channel, leading to rapid influx of chloride ions and subsequent hyperpolarization of the membrane potential, thus inhibiting the cells ability to react to another action potential (Sigel and Steinmann, 2012). In contrast, $GABA_B$Rs are metabotropic, G_i-protein coupled receptors, that mediate slower responses through second messengers acting on G-protein activated inwardly rectifying K^+-channels (GIRKs). The opening of these channels leads to the efflux of K^+ ions from the neuron, which in turn hyperpolarizes the membrane. Moreover, $GABA_B$Rs are also located on the presynaptic membrane and have an autoregulatory role, thereby blocking forthcoming GABA release (Gassmann and Bettler, 2012). One regulatory mechanism the receptors exhibit is the modulation of DA release within the striatum. Generally, MSNs located in the striatum are GABAergic projection neurons, which project to certain nuclei within the basal ganglia and govern the pathways to voluntary movement in cooperation with DA, as described before. Within the striatum, DA axons have been found to possess $GABA_A$Rs as well as $GABA_B$Rs, which are modulated by GABA in a way that DA release is being tonically inhibited. This GABA signal is mediated through MSNs (Lanciego, Luquin and Obeso, 2012; Lopes *et al.*, 2019), with additional implications of DA GABA co-release described later.

Ultimately, signaling is terminated by the uptake of the neurotransmitter through GATs, most importantly GAT1 but also GAT2, GAT3 or BGT1 (betaine/GABA transporter). Thereafter, GABA is either recycled and packaged into synaptic vesicles or

degraded through different enzymes, with its metabolites finally contributing to the energy metabolism through the TCA cycle (Roth and Draguhn, 2012).

1.3.2 GAT1 structure and transport mechanism

Several neurotransmitter transporters have been identified through homology cloning, leading to the discovery of a plethora of Na^+/Cl^-dependent plasma membrane-associated transporters which translocate substrates like dopamine or GABA, among others (Chen, Reith and Quick, 2004). Most of those transporters, including GAT1, are classified as neurotransmitter sodium symporters, which belong to the SLC6 family (Focke, Wang and Larsson, 2013).

GAT1 transport activity is driven by the inwardly-driected Na^+ electrochemical gradient established throughout the membrane by the Na^+/K^+-ATPase (Scimemi, 2014). Kinetic studies have established the transport stoichiometry of GAT1 to be two Na^+, 1 Cl^- and 1 GABA molecule, revealing alternating conformational changes during the transport process (Lu and Hilgemann, 1999; Loo *et al.*, 2000). An outward-open facing conformation allows the binding of sodium ions and the substrate and additional transported ions, whereas the switch to inward-facing leads to the release of all molecules into the cytoplasmic space (Kristensen *et al.*, 2011).

Generally, GAT1 adopts the canonical LeuT-fold, which is a bacterial homologue of many members of the SLC6 family and is expressed as a 12 transmembrane domain (TMD) structure (**Figure 3**). Altogether, the protein is comprised of two related helical pseudo-repeats, namely TMD 1 – TMD 5 as well as TMD 6 – TMD 10, including the N- and C-terminus being located on the intracellular space (Yamashita *et al.*, 2005). TMD 1 and TMD 6 contain unwound regions, which connect the subparts TMD 1a and b as well as TMD 6a and b, and together with TMD 3 and 8 build the inner core of the substrate and ion binding pocket (Zafar and Jabeen, 2018). The identified TMDs being most important for conformational changes during transport involve 1, 2 and 6 as well as extracellular loop 4 (EL4) which mediates closure and opening of the gate to the extracellular space. The transition into the inward-open state is conducted through TMD 1, 2, 5, 6 and 7 through hinge-bending, disrupting the sodium binding sites and therefore leading to substrate and ion

release (Krishnamurthy and Gouaux, 2012). Especially TMD 1a was found to open up the cytosolic pathway from the central pocket for release by unwinding and bending (Zhu *et al.*, 2023). Lastly, through studying the selective GAT1 inhibitor tiagabine, it was determined that the drug locks the transporter in an inward-open conformation by interfering with the substrate release pathway which ultimately leads to the inhibition of GABA uptake (Motiwala *et al.*, 2022).

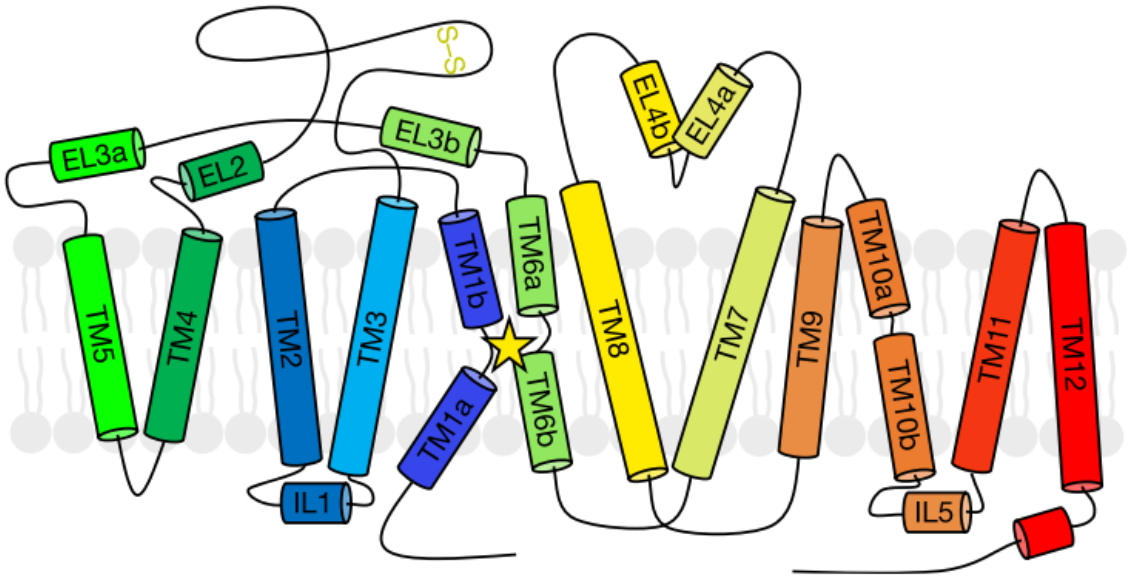

Figure 3 Illustration of SLC6 family transporter structure, exemplified by full-length hGAT1. *The topology comprises 12 TMDs, with the star depicting the binding pocket governed by TMD 1, 3, 6 and 8. Reproduced from Motiwala, Z. et al. (Nature, 2022) with permission from Springer Nature. License number: 6198910538205.*

1.3.3 GABA co-release in dopaminergic neurons

As discussed above, the presence of GABAergic markers in rodent and human midbrain DA neurons, such as VGAT and GAT1, has been confirmed through different reports (Poulin *et al.*, 2014; Conrad *et al.*, 2024; Srinivasan *et al.*, 2025). However, when addressing GABA co-release in DA neurons, there is evidence that, rather than VGAT, VMAT2 is responsible for packaging GABA into synaptic vesicles for co-release (Tritsch, Ding and Sabatini, 2012). Structurally viewed, GABA as a zwitterionic amino acid, is fairly different in comparison to typical substrates of VMAT2 (Zheng, Dwoskin and Crooks, 2006; Zhang *et al.*, 2024). Nevertheless, GABA was still found to co-localize with VMAT2-positive, but VGAT-negative synaptic vesicles

in DA neurons (Stensrud, Purchades and Gundersen, 2014). Additionally, through radioligand flux assays, GABA was found to reduce the uptake of VMAT2 substrates, thus implying GABA to be a VMAT2 substrate (Srinivasan *et al.*, 2025).

But the mechanism with which GABA is obtained within DA neurons for release is seemingly not dependent on GADs as known from the classical GABA synthesis mechanism, due to low levels of expression of the enzymes in DA neurons (Kim *et al.*, 2015; Tritsch, Granger and Sabatini, 2016). On the one hand, DA neurons were found to rely on extracellular GABA uptake through GAT1. The selective deletion of GAT1 as well as VMAT2 from SNc DA neurons lead to the complete abolishment of GABA co-transmission, showing the importance of both transporters within this pathway (Tritsch *et al.*, 2014; Melani and Tritsch, 2022). Alternatively, a non-canonical synthesis mechanism involving ALDH1A1, an enzyme known to be expressed in DA neurons, includes another possible way of acquiring GABA through putrescine (Kim *et al.*, 2015).

There is evidence for an autoregulatory role of GABA co-release from striatal dopamine terminals, where GABA is able to mitigate phasic DA release through the stimulation of $GABA_AR$s. This autoregulatory inhibition was lost when GAT1 was conditionally knocked out in mice (Patel *et al.*, 2024). Accordingly, there is a suggestive function of GABA co-release contributing to DA synapse maintenance in the striatum. After initiating two PD models through injecting PD-neurotoxins, GABAergic signaling diminished significantly as early as 1 day after injection, whereas DA transmission lasted several days to weeks until the synapse degeneration commenced (Kim *et al.*, 2023). Together, those reports point towards a relevant physiological role of GABA co-release in DA synapse maintenance and autoregulation, with an emphasis on GAT1 for overall functionality of these pathways.

1.3.4 GAT1-G63S mutation

GAT1 is encoded by the *SLC6A1* gene, with its main function within the healthy brain, being the uptake of extracellular GABA to halt the neurotransmitter's inhibiting effects by lowering its concentration in the extracellular space (Scimemi, 2014). Additionally, GAT1 has implications in being crucial for GABA co-release in DA

neurons and mediating autoregulatory mechanisms in DA synapses (Patel *et al.*, 2024). On the other hand, there are several *SLC6A1*-related diseases, which have been associated with a wide variety of mainly loss-of-function mutations, thus leading to various neurological disorders (Shah *et al.*, 2024). Especially epilepsy, developmental and cognitive impairments, as well as autistic traits were found to be the most frequently emerging clinical appearances (Goodspeed *et al.*, 2020). Moreover, in a study where 22 different *SLC6A1* variants were investigated, the results suggested that endoplasmic reticulum retention of the transporter, following a reduction in surface expression and therefore activity, and complete loss of transporter function were the major pathophysiological mechanisms across all researched variants (Mermer *et al.*, 2021).

Only recently, a *de novo* mutation in a parkinsonian patient has been found in GAT1, who presented with bilateral dopaminergic neurodegeneration and globus pallidus lesions. Whole genome sequencing revealed a missense mutation, where the glycine at position 63 was substituted with a serine ($GAT1^{G63S}$) (Leclert *et al.*, 2024). However, it is not fully clarified whether the variant is directly related to the patient's parkinsonian syndrome.

G63 is found in the unwound region of TMD1 as a conserved structure throughout all four GABA transporter subtypes (Kristensen *et al.*, 2011). More specifically, it is situated within the substrate binding pocket, where it was found to not directly bind to the ligand, but rather interact with the Na^+-ions which are being co-transported with GABA into the cell (Skovstrup *et al.*, 2010; Baglo *et al.*, 2013). Additionally, it has been found to play a crucial role in stabilizing local conformations by forming hydrogen bonds to neighboring structures (Zhu *et al.*, 2023). Interestingly, it has been reported previously, that the G63S mutant lead to a loss of sodium-dependent GABA currents as well as complete [^{3}H]-GABA uptake abolishment (Kanner, 2003), indicating that G63 holds an important role in efficient transporter functionality.

2 Aim

Considering all the mentioned facts about DA neuron vulnerability and neurotransmitter co-release, the role of GABA signaling in physiology and disease is still underexplored. Through the discovery of the *de novo* mutation GAT1^{G63S} in a parkinsonian patient presenting with DA neurodegeneration (Leclert *et al.*, 2024) and the transporters increasing relevance in GABA co-release in DA neurons (Tritsch *et al.*, 2014), a new research perspective has emerged, spotlighting how altered GABA homeostasis may contribute to increased DA vulnerability. Therefore, the aims are summarized as follows:

- Investigate the transport function and localization of the human GAT1 (hGAT1)^{G63S} variant in HEK293 cells.
- Generate and thereafter test hGAT1^{WT} and hGAT1^{G63S} for functionality.
- Produce and test hGAT1-adeno-associated viruses (AAVs) in TSA201 cells for future *in vivo* studies.

Accordingly, the transport action of the hGAT1^{G63S} was studied by measuring [^{3}H]-GABA uptake through radioligand uptake assays in HEK293 cells compared to hGAT1^{WT}. Additionally, the localization of the transporters within the cells was determined by performing a membrane staining using trypan blue and subsequent confocal imaging. To be able to investigate the impact of the mutant *in vivo*, constructs have been subcloned into a Cre-dependent pAAV-vector and tested for their transporter functionality, as well as Cre-dependence through co-expression with Cre recombinase.

3 Materials and Methods

3.1 Cell culture

Human embryonic kidney (HEK) 293 as well as TSA (transformed HEK293) 201 cells were cultured and maintained in Dulbecco's Modified Eagle Medium (DMEM) High Glucose (Biowest, L0102-500) supplemented with 10% fetal bovine serum (FBS, Capricorn Scientific, FBS-11A) and 1% Penicillin-Streptomycin (P/S, Sigma-Aldrich, P4333). All cell lines were grown in a humidified 5% CO_2 atmosphere at 37°C.

3.2 Trypan Blue Staining

HEK293 cells were plated in a 6-well plate in order to reach 60 - 80% confluency the next day. Thereafter, the cells were transfected with either eYFP-hGAT1^{WT} or eYFP-hGAT1^{G63S} (**Figure 4A and B**) plasmid using Lipofectamine® 2000 Transfection Reagent (Invitrogen, 11668-019) according to the manufacturer's protocol. Simultaneously, 4 wells of two µ-Slide 8-well plates (Ibidi, 80826) each were coated with poly-D-Lysine (PDL, Sigma-Aldrich, P1149, 1 mg/ml) and incubated overnight (o/n) at 37°C. The following day, 30,000 – 50,000 transfected cells were seeded into designated, pre-coated wells and once again incubated o/n at 37°C. Cells were then first washed once with Krebs-HEPES buffer (KHB; 10 mM HEPES, 120 mM NaCl, 3 mM KCl, 2 mM CaCl2.2H2O, 2 mM MgCl2.6H2O, 20 mM D-(+)-Glucose-Monohydrate, pH 7.3). After the KHB removal, a Trypan blue (Sigma-Aldrich, RNBL1608) 0.05% solution in phosphate-buffered saline (PBS; 2.7 mM KCl, 1.5 mM KH2PO4, 137 mM NaCl, 4.3 mM Na2HPO4.2H2O, pH 7.3) was added into the wells and incubated for 10 minutes at 37°C. Thereafter, the cells were washed again with KHB once and subsequently imaged with a Nikon confocal microscope using a 60x objective.

A

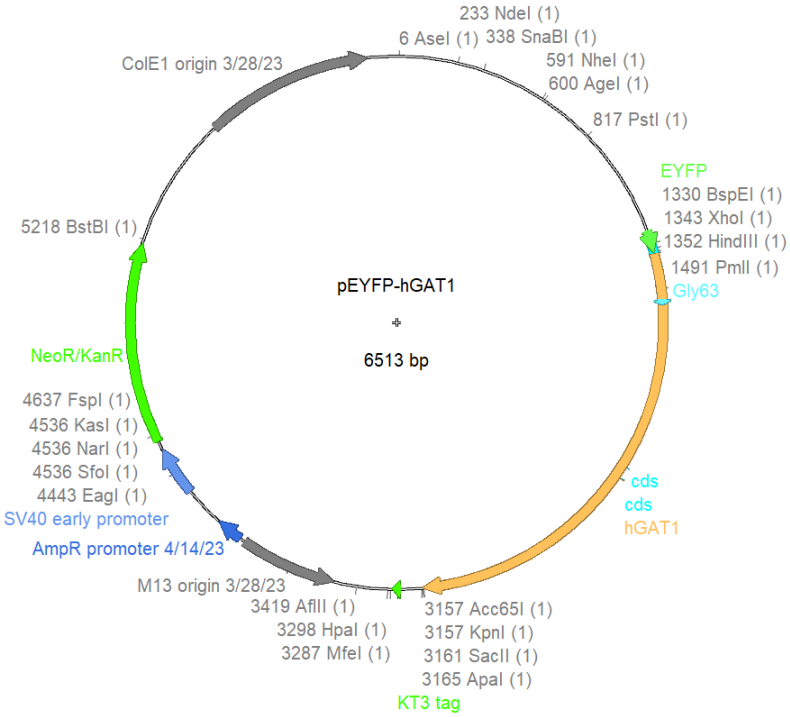

B

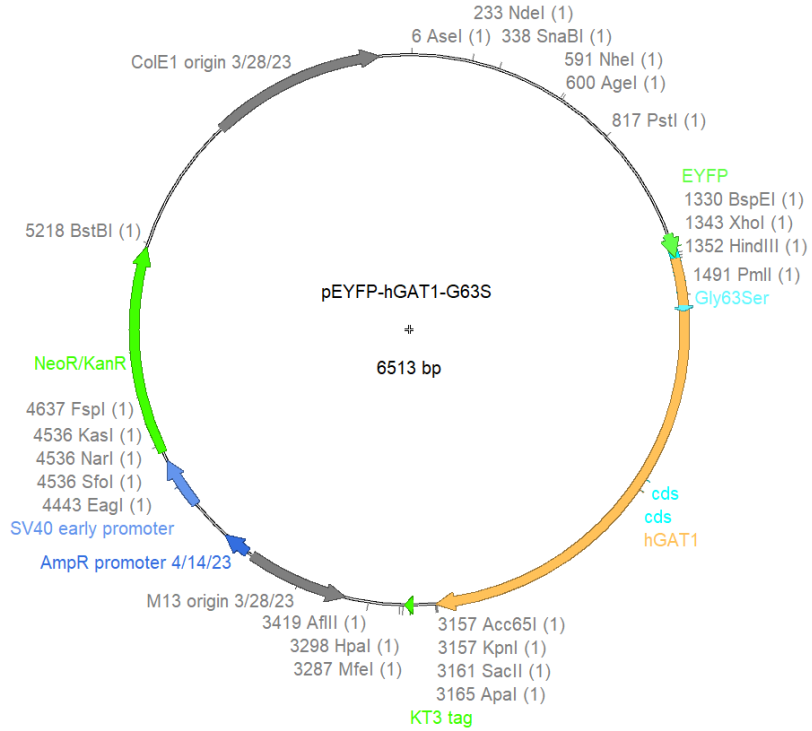

Figure 4 Plasmid maps of (A) eYFP-hGAT1^{WT} and (B) eYFP-hGAT1^{G63S}. *The constructs encode (A) the human GAT1 and (B) the G63S mutated human GAT1, including an eYFP-tag for visualization and a kanamycin resistance for bacterial selection. Restriction enzyme sites are also presented on the map. Images were obtained from ApE.*

3.3 Radioligand Uptake Assays

HEK293 and TSA201 cells were seeded in 6-well plates in order to reach 60 – 80% confluency the following day. HEK293 cells were then transfected with the before-mentioned plasmids (**Figure 4A and B**) using Lipofectamine® 2000 Transfection Reagent. TSA201 cells were transfected with pAAV-Syn1-DIO-hGAT1 (cre-off) (pAAV-DIO-hGAT1^{WT} cre-off) (**Figure 5**) and pAAV-Syn1-DIO-hGAT1^{G63S} (cre-off) (pAAV-DIO-hGAT1^{G63S} cre-off) using Polyethylenimine (PEI, Sigma-Aldrich, 97H04121; 1 mg/ml, pH 7). For that, plasmids were added to serum-free DMEM and incubated together with PEI for 15 min at room temperature (RT), where the amount of PEI corresponded to three times the total mass of DNA. The DNA-PEI solution was added dropwise to the cells and incubated o/n at 37°C. The next day, cells were split into PDL-coated 48-well plates and once again incubated o/n at 37°C.

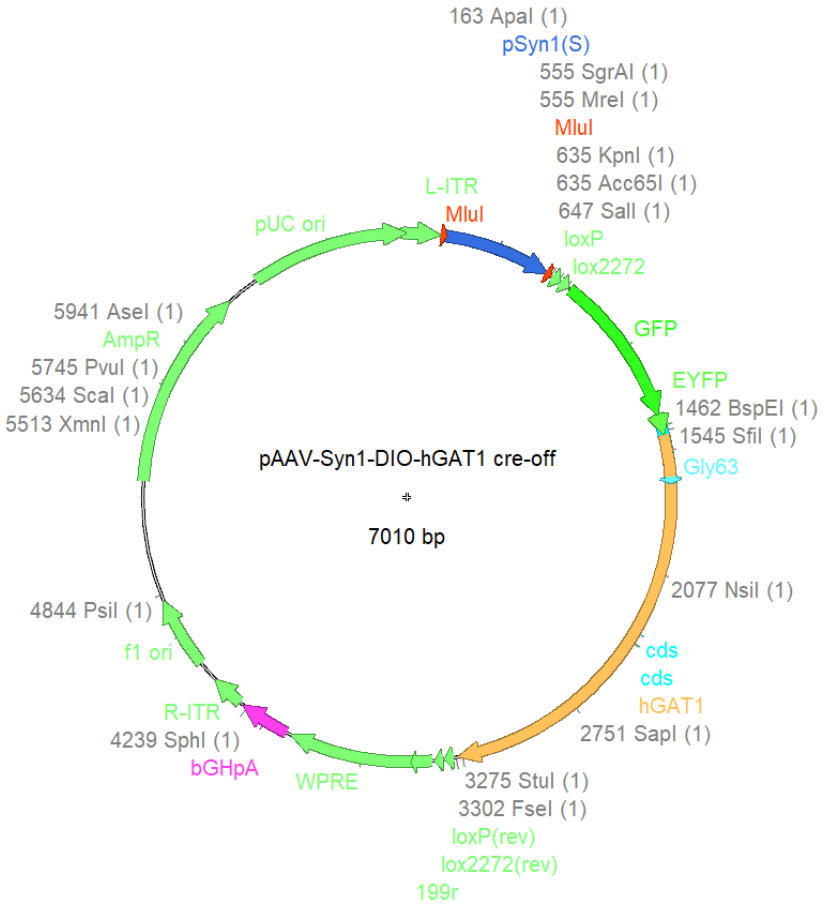

Figure 5 Plasmid map of pAAV-Syn1-DIO-hGAT1^{WT} (cre-off). *The construct encodes the human GAT1, which is fused to an eYFP-tag and under the control of the Synpasin 1*

promoter in a cre-off configuration. It includes a DIO cassette, flanking hGAT1 with loxP and lox2272 sites, which in the presence of a Cre-recombinase, would be inverted and transcriptionally inactivate the transgene. Further included are ITRs needed for viral packaging, restriction enzyme sites and an ampicillin resistance for bacterial selection. Image was obtained from ApE.

The next day, the uptake assay was performed in triplicates for each plasmid, with the first column being used for the specific uptake with 50 nM [^{3}H]-GABA (Revvity, 3344742, 1 mCi/ml, 75 Ci/mmol) in RT KHB, the second for the nonspecific uptake with 10 µM tiagabine, a selective inhibitor of GAT1 (Motiwala *et al.*, 2022), (abcr, AB436617) in RT KHB and the last one for counting cells, as schematically showcased in **Figure 6**. First, all wells were washed with KHB at room temperature, before initiating the specific uptake by adding [^{3}H]-GABA in KHB to each well of the first column in 10 second intervals. After an exact 3-minute incubation at RT, the reaction was stopped rapidly by washing each well three times with ice cold KHB. Thereafter, to the second column for the nonspecific uptake, tiagabine in KHB was added to incubate for 5 minutes at RT. Then, to each well in 10 second intervals, [^{3}H]-GABA together with tiagabine were added, left to incubate for 3 minutes at RT and then again washed three times with ice cold KHB as described before. To lyse the cells, 1% sodium dodecyl sulfate (Sigma-Aldrich, SDBB3638) was added to each well and the lysates were transferred into vials containing 2 ml of scintillation cocktail (ROTISZINT®Routine, Carl Roth). To measure the total activity, 10 µl of the 50 nM [^{3}H]-GABA solution was added to 3 different scintillation vials in a 1:200 dilution and [^{3}H]-GABA cell uptake was measured via liquid scintillation counting by a Packard Tri-Carb 2300 TR liquid scintillation analyzer. Finally, the wells in the last column were once washed with RT KHB, before trypsin (Sigma-Aldrich, T3924) was added. The cells were then triturated using a pipette and counted using a Neubauer hemocytometer (Marienfeld Superior).

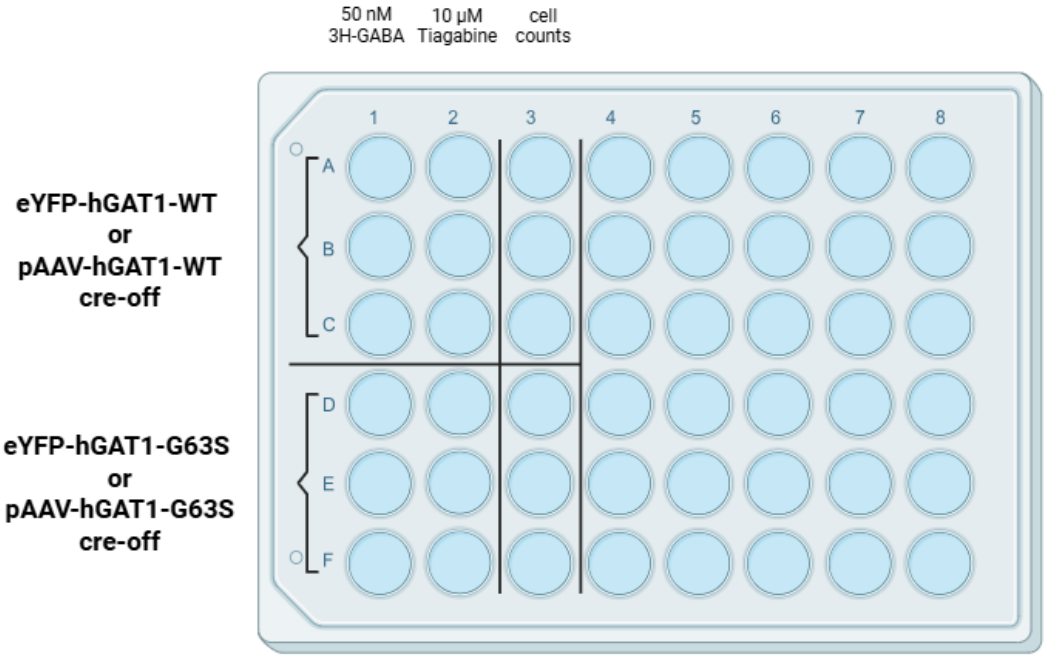

Figure 6 Schematic illustration of the set-up for the radioligand uptake assay. *HEK293 and TSA201 cells were transfected with either WT or mutated plasmids in triplicates. The cells were incubated with 50 nM [^{3}H]-GABA in the first column and in the second column, firstly treated with 10 µM tiagabine before adding [^{3}H]-GABA. The last column was left for cell counting. Image was obtained from BioRender.*

3.4 Cloning

To start the cloning process, firstly the DNA of interest had to be amplified using the polymerase chain reaction (PCR) method. While strictly working on ice during the whole procedure, different components for each plasmid were combined, as follows: CloneAmp™ HiFi PCR Premix (Takara, 2407B34A), 10 µM forward primer (eYFP_fw ATGGTGAGCAAGGGCGAGGA), 10 µM reverse primer (hGAT1_rv CTAGATGTAGGCCTCCTTGCTG), 50 ng/µl eYFP-hGAT1^{WT}, 25 ng/µl eYFP-hGAT1^{G63S} (**Figure 4A and B**) and nuclease free water. A Labnet MultiGene™ thermal cycler was programmed for 30 seconds at 98°C for the initial denaturation, followed by 30 cycles of 10 seconds at 98°C for further denaturation, 30 seconds at 68°C for annealing, 1 minute and 30 seconds at 72°C for extension and additional 5 minutes at 72°C for the termination of the reaction. The PCR products were then inspected by gel electrophoresis using a 1.5% (w/v) agarose (BioCat, AGA500-BCAT) gel in TAE buffer (40 mM Tris, 20 mM acetic acid and 1 mM EDTA, pH 8.5)

at 120 Volt (V) for 1 hour. The samples were prepared with Gel Loading Dye Purple (NEB, 10208667) in a 1:6 ratio and as a marker a 1 kb DNA ladder (NEB, 10267246) was used. The PCR products were cleaned up using the NucleoSpin® Gel and PCR Clean-up kit (Macherey-Nagel, 740609,250) according to manufacturer's protocol.

Thereafter, a restriction enzyme digest was performed, by using AscI (NEB, 10145410) as the restriction enzyme. In separate tubes, the PCR products and the vector, pAAV-Syn1-DIO-hDAT (cre-off) (hDAT cre-off) (**Figure 7**), (1µg/ml) were assembled, while working on ice, as follows: rCutSmart™ Buffer (NEB, 10118973) in a 1:10 ratio, nuclease-free water and restriction enzyme. The tubes were incubated at 37°C for 1 hour and the digestion was heat-inactivated for 20 minutes at 80°C. To the vector, before heat-inactivation, Quick CIP (NEB, 10016577) was added, and incubated an additional 10 minutes at 37°C. To separate the digested bands, a second 1.5% agarose gel was prepared, and gel electrophoresis was performed the same way as described before. The respective bands, being the vector backbone and inserts, were then cut out of the gel using a scalpel. Subsequently the NucleoSpin® Gel and PCR Clean-up kit was used according to manufacturer's protocol. The concentrations of the purified vector and inserts were measured using Nanodrop.

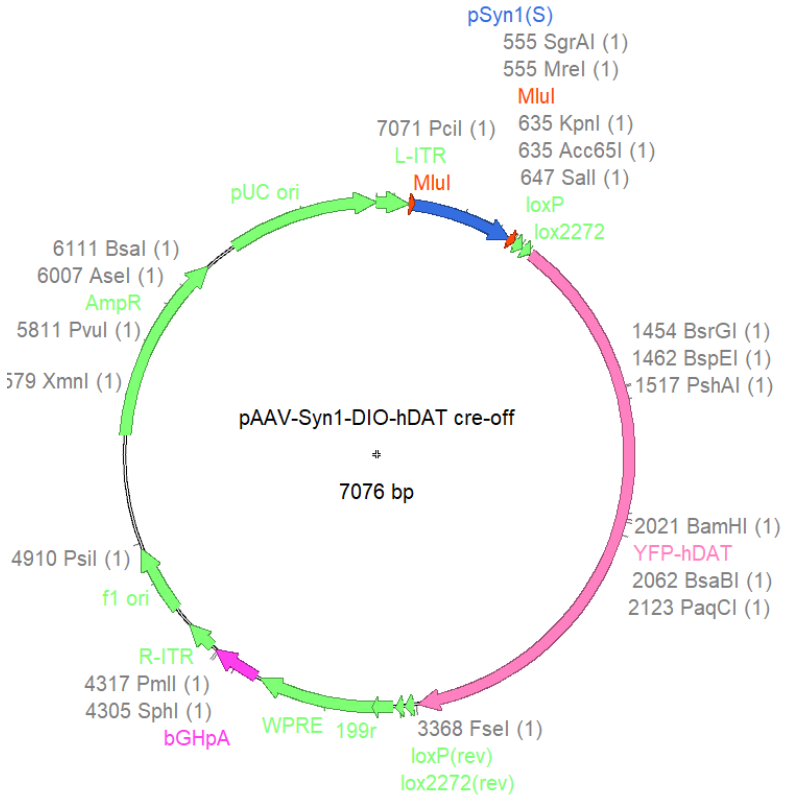

Figure 7 Plasmid map of pAAV-Syn1-DIO-hDAT (cre-off). *The construct encodes the human DAT, which is fused to a YFP-tag under the control of the Synpasin 1 promoter in a cre-off configuration. It includes a DIO cassette, flanking hDAT with loxP and lox2272 sites, which in the presence of a Cre-recombinase, would be inverted and transcriptionally inactivate the transgene. Further included are ITRs needed for viral packaging, restriction enzyme sites and an ampicillin resistance for bacterial selection. The image was obtained from ApE.*

Lastly, the inserts and vector were ligated together in a 3:1, 1:1 and 0:1 ratio, respectively. For that, a T4 DNA ligase (NEB, M0202S) was used and combined, while working on ice, with T4 DNA ligase buffer (NEB, 10023774) in a 1:10 ratio and nuclease-free water was added. Tubes were incubated for 10 minutes at RT and heat-inactivated at 65°C for 10 minutes. The ligated products were then used to transform XL1-blue competent bacteria. The cloning success was determined by Sanger sequencing.

3.5 Cre-configuration testing

TSA201 cells were seeded in a 24-well plate in order to reach 60 – 80% confluency the next day. In order to test the newly cloned plasmids and their cre-configuration, cells were transfected via PEI using the following plasmids: pcDNA3.1-Cre-mCherry (Cre-mCherry), pAAV-Syn1-DIO-hGAT1 (cre-on) (pAAV-DIO-hGAT1^{WT} cre-on) (**Figure 8A**), pAAV-DIO-hGAT1^{WT} cre-off, pAAV-Syn1-DIO-hGAT1^{G63S} (cre-on) (pAAV-DIO-hGAT1^{G63S} cre-on) and pAAV-DIO-hGAT1^{G63S} cre-off, including pAAV-Syn1-DIO-hDAT (cre-on) (hDAT cre-on) (**Figure 8B**) and hDAT cre-off as controls.

A

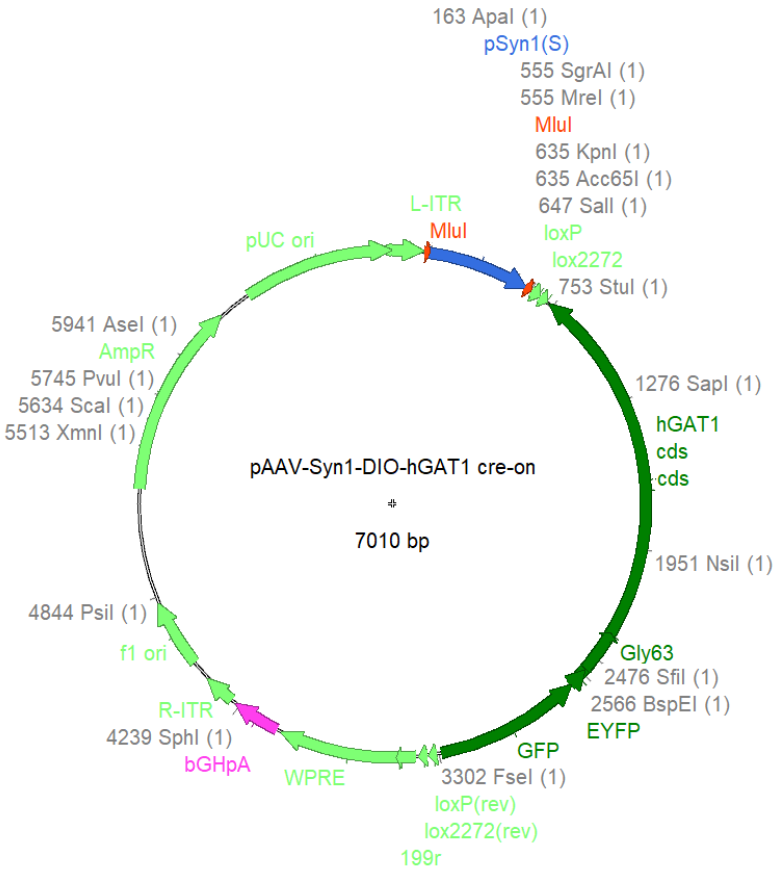

B

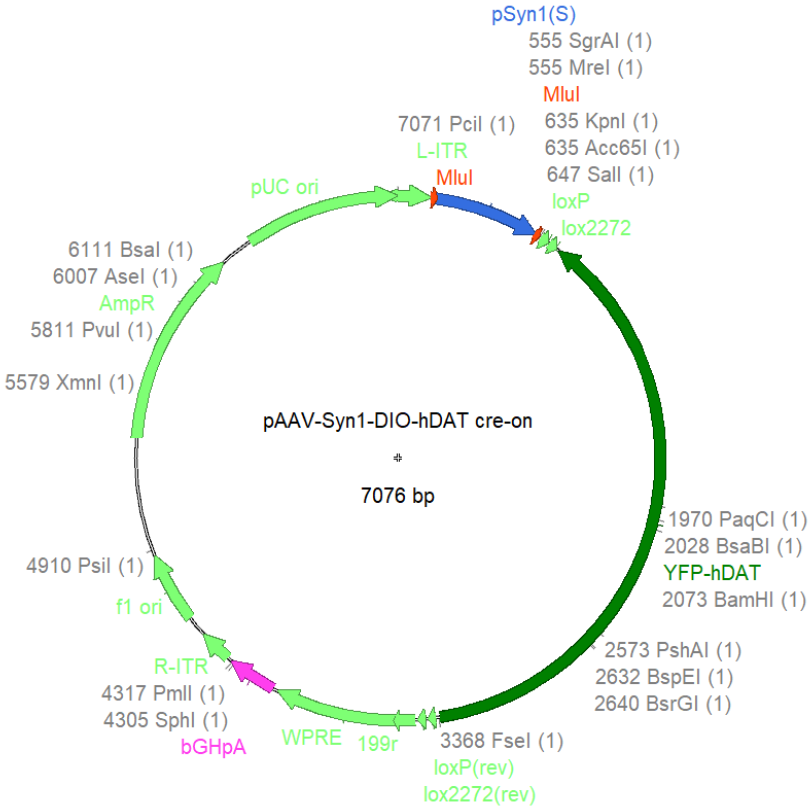

Figure 8 Plasmid maps of (A) pAAV-Syn1-DIO-hGAT1^{WT} (cre-on) and (B) pAAV-Syn1-DIO-hDAT (cre-on). *The constructs encode (A) the human GAT1, which is fused to an eYFP-tag and (B) the human DAT, which is fused to a YFP-tag, under the control of the Synpasin 1 promoter in a cre-on configuration and therefore in a cre-dependent manner. They include a DIO cassette, flanking the transgenes with loxP and lox2272 sites, which in the presence of a Cre-recombinase, would be inverted and transcriptionally activate the transgenes. Further included are ITRs needed for viral packaging, restriction enzyme sites and ampicillin resistance for bacterial selection. Images were obtained from ApE.*

TSA201 cells were transfected with single plasmids as well as in combination with cre-mCherry. The transfection plan is schematically presented in **Figure 9**. Images were taken with a fluorescence microscope using a 20x objective.

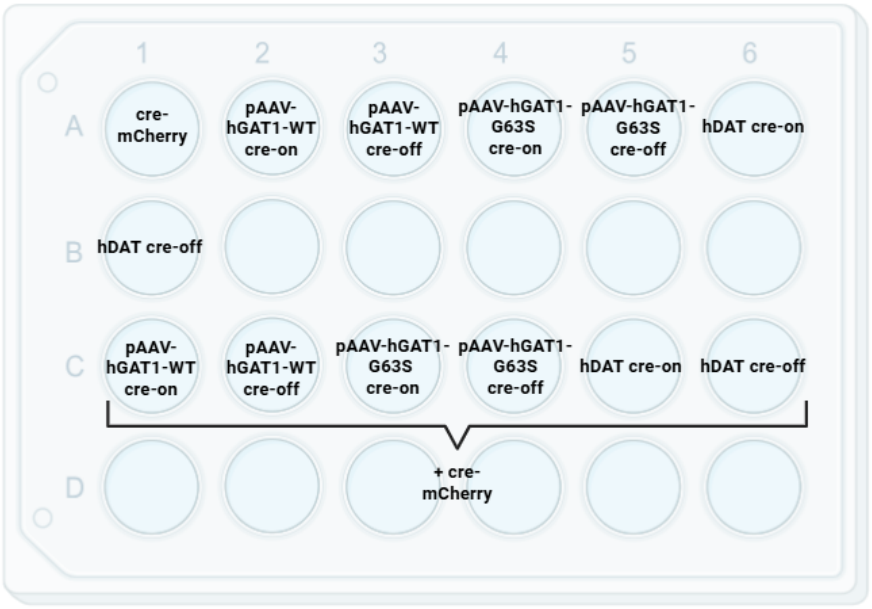

Figure 9 Schematic illustration of the set-up for the cre-configuration testing. *TSA201 cells were transfected with a different subset of plasmids, either as single plasmids per well or in combination with cre-mCherry. Image was obtained from BioRender.*

3.6 Adeno-associated virus production and extraction

TSA201 cells were seeded in a T-175 flask in order to reach 60 – 80% confluency over the weekend. Thereafter, cells were transfected with the viral plasmids pAdenoHelper and pAAV-DJ (**Figure 10A and B**), as well as the plasmids hDAT cre-off (**Figure 7**), pAAV-DIO-hGAT1^{WT} cre-on (**Figure 8A**) and pAAV-DIO-hGAT1^{G63S} cre-on, using PEI as previously described. After 24 hours, the medium was exchanged by adding 3 ml of the old medium to 27 ml serum-free OptiPRO™ (gibco, 12309-019) with 1% P/S. The cells were then incubated for 72 hours at 37°C and checked on daily under a fluorescence microscope.

A

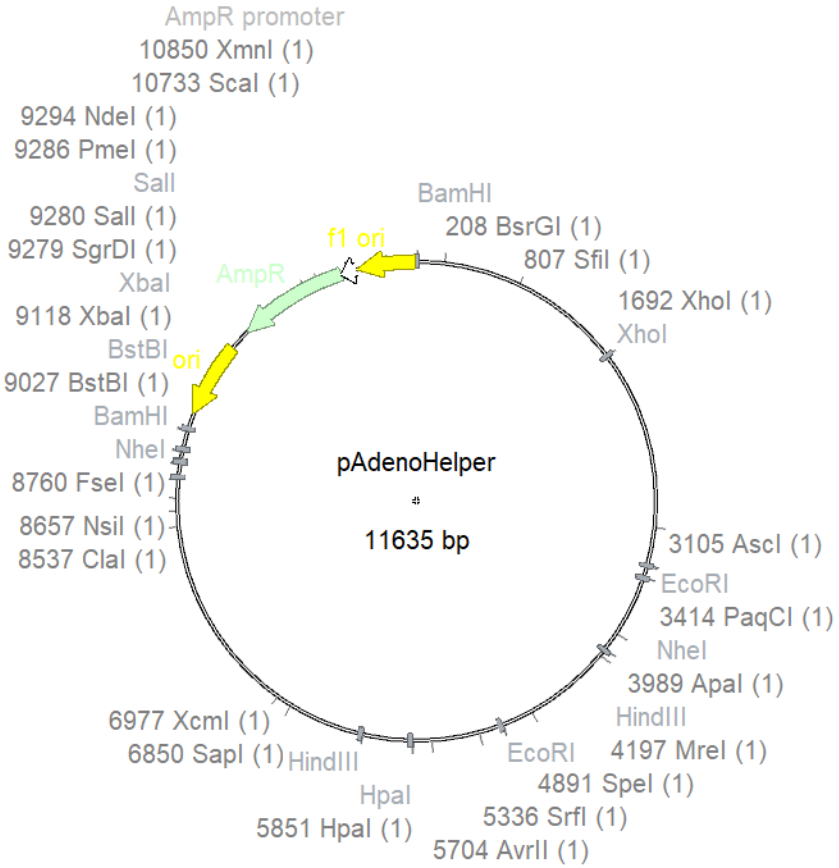

B

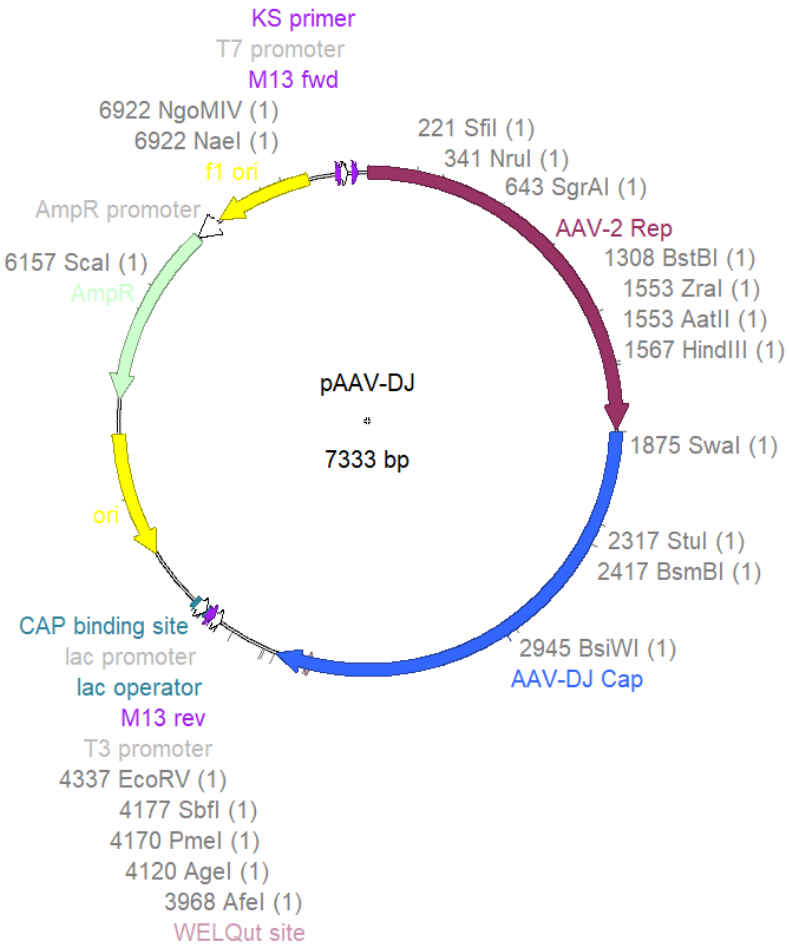

Figure 10 Plasmid maps of (A) pAdenoHelper and (B) pAAV-DJ. *The constructs encode the (A) AAV helper genes, as well as (B) AAV replication and capsid genes. Both are contributing to and needed for the packaging of pAAV-plasmids with ITRs into viral vectors. Shown are also restriction enzyme sites and an ampicillin resistance for bacterial selection. Images were obtained from ApE.*

After 72 hours, before the virus was extracted, about 200 µl of medium was taken out of the T-175 flask and kept at 4°C, which was used for later testing. Cells were then removed mechanically by a cell scraper, transferred into a falcon tube and centrifuged at 2000 g for 15 minutes at RT. The supernatant was discarded, and the cell pellet fully resuspended in 1 ml lysis buffer (300 mM NaCl, 50 mM Tris-HCl, pH 8.5), which was then transferred into a 1.5 ml Eppendorf tube. To extract the virus fully from the cells, a freeze-thaw cycle was performed for a total of three times. Firstly, the 1.5 ml Eppendorf tube containing the cell suspension was put into liquid nitrogen for 10 minutes. Thereafter, the tube was transferred into a 37°C-hot water

bath and kept there for another 10 minutes. Lastly, the tube was vortexed for 10 seconds and the cycle was repeated. Once all cycles were completed, 1 µl Benzonase Nuclease (Sigma-Aldrich, 8263-5KU) was added to the cells, vortexed and incubated for 1 hour at 37°C. The cells were then centrifuged at 14,000 g for 15 minutes at RT and the supernatant was harvested using a 5 ml syringe and 19G needle. The supernatant was then filtered through a 0.45 µm filter and the virus collected. Immediately after extraction, different concentrations of the virus were tested out by transducing TSA201 cells. In the case of Cre-on constructs, TSA201 cells were first transfected with a plasmid that comprises a Cre-recombinase by using PEI. Once the virus was added, the cells were incubated for 72 hours at 37°C. Images were acquired with a fluorescence microscope using 10x and 20x objectives.

3.7 Sequencing

The success of the cloning process of pAAV-DIO-hGAT1^{WT} and ^{G63S} cre-off and -on, was determined through sequencing of these plasmids by Sanger sequencing. For that, the plasmids were used to transform XL1-blue competent *E. coli* through heat shocking them for 30 seconds at 42°C and subsequently incubating the bacteria in SOC medium (Thermo Fischer, 15544034) at 37°C for 1 hour while shaking. Thereafter, the bacteria were plated on LB agar plates including ampicillin (50 mg/ml) and incubated at 37°C for 16 hours. The next evening, single colonies for every plasmid were picked and incubated in LB medium (for 1 L: 171 mM NaCl, 1% (w/v) Tryptone, 0.5% (w/v) yeast extract, pH 7) with ampicillin in a 1:1000 ratio at 37°C for 16 hours while shaking.

To extract the plasmids, a miniprep was performed using the NucleoSpin® Plasmid kit (Macherey-Nagel, 2409-004) according to manufacturer's protocol and concentrations were measured using Nanodrop. In order to identify the different Cre-configurations, a restriction enzyme digest was performed, as described before, using PstI-HF® (NEB, 10163616). Thereafter, the samples were examined by gel electrophoresis, as described before. As a negative and positive control, undigested and digested hDAT cre-off, respectively, have been used. After confirmation of positive

clones, selected samples were prepared to be sent to Microsynth (Balgach, Switzerland) for Sanger sequencing using the primer hSyn1_fw, GAG-TCGTGTCGTGCCTGAGA.

Thereafter, the miniprep samples were used for retransforming the same competent bacterial cells, which were handled alike as described before. For extraction of the plasmids, a midiprep was performed using the NucleoBond® Xtra Midi Plus kit (Macherey-Nagel, 2409-003) according to manufacturer's protocol. Those samples were also sent to Microsynth for sequencing, using the beforementioned primer.

3.8 Data analysis

For analyzing the [^{3}H]-GABA uptake assay, the counts per minute (cpm) were determined by subtracting the counts of the nonspecific uptake, representing the background, and multiplying the outcome by the concentration factor, which is calculated by dividing the total substrate concentration by the radiolabeled substrate concentration. The normalization of the counts was conducted through division of the multiplication of the reaction time, total activity of the reaction and the cell counts, which resulted, in this case, in [^{3}H]-GABA uptake per pmol per million cells per minute. For the calculations, Microsoft Excel was used, and statistical significance was determined by applying the two-tailed unpaired Student's t-test (significance level < 0.05) in GraphPad Prism.

4 Results

4.1 Uptake activity and localization of hGAT1^{G63S} in HEK293 cells

To test the transporter activity of hGAT1^{G63S} (**Figure 4B**), HEK293 cells were transiently transfected with either hGAT1^{WT} or the mutant variant and a radioligand uptake assay was performed using [^{3}H]-GABA.

Only recently, the *de novo* GAT1 mutant, G63S, was discovered in an individual who presented with a parkinsonian syndrome and bilateral DA neurodegeneration (Leclert *et al.*, 2024). A previous biochemical report stated that hGAT1^{G63S} led to complete abolishment of [^{3}H]-GABA uptake, indicating that this position within the transporter plays an important role in GABA transport activity (Kanner, 2003). Since GAT1 is crucial for GABA reuptake and GABA co-release from DA neurons (Tritsch *et al.*, 2014; Kim *et al.*, 2023; Patel *et al.*, 2024), we speculated that hGAT1^{G63S} may alter GABA co-release from DA neurons.

I was able to confirm, that the uptake of [^{3}H]-GABA was fully abolished in hGAT1^{G63S} transfected cells in comparison to hGAT1^{WT} (**Figure 11A**). This outcome is in line with a previous finding (Kanner, 2003).

To make sure that the variant, rather than other factors, was the reason for the transport dysfunction, a trypan blue staining on transfected HEK293 cells was performed to visualize whether the transporter was present in the plasma membrane. A frequent reason for reduced or failed uptake activity through GAT1 mutants, among others, was shown to be the retention of the protein within the secretory pathway (Farhan *et al.*, 2007, 2008). In my experiments, I found that hGAT1^{G63S} was indeed present on the cell surface, as judged by the co-localization of its eYFP-N-terminal tag with the trypan blue stained plasma membrane (**Figure 11B**)**.** Together, these outcomes indicate that, although being transported to the cell membrane, hGAT1^{G63S} must have failed to transport GABA, its substrate.

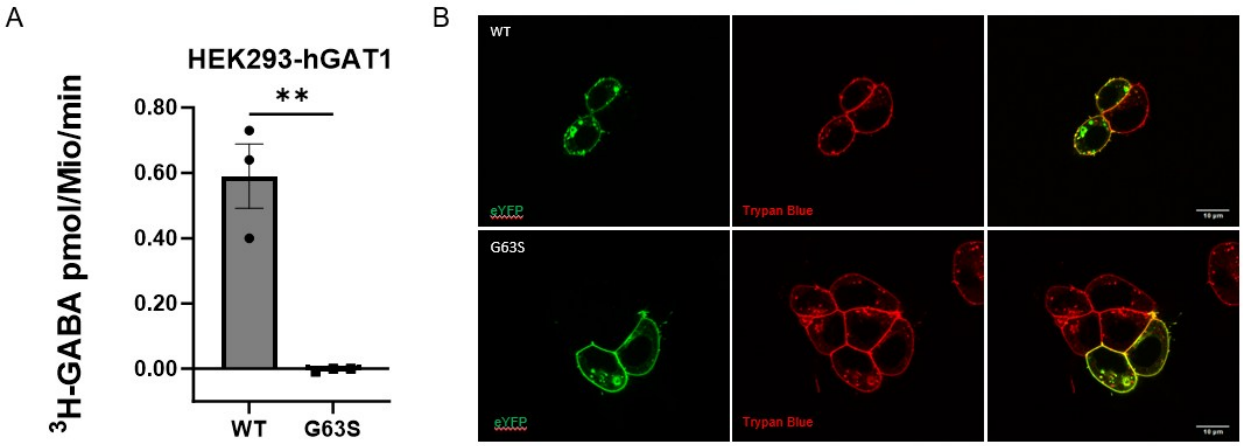

Figure 11 hGAT1^{G63S} fails to transport GABA, albeit being trafficked to the cell surface. (A) *Measurement of [^{3}H]-GABA uptake in HEK293 cells transfected with hGAT1^{WT} or hGAT1^{G63S}. Specific and nonspecific uptake were measured with 50 nM [^{3}H]-GABA and presence of 10 µM tiagabine, respectively. Error bars show ± SEM from n = 3 biological replicates analyzed with two-tailed unpaired Student's t-test. * p<0.05, ** p<0.01, *** p<0.001, **** p<0.0001* ***(B)*** *Representative confocal images of HEK293 cells transfected with hGAT1^{WT} or hGAT1^{G63S}. The green signal represents the eYFP tagged hGAT1, whereas the red signal shows the trypan blue-stained plasma membrane. An overlap of both signals displays the localization of hGAT1 on the plasma membrane.*

4.2 Uptake activity and Cre-configuration testing of pAAV-Syn1-DIO-hGAT1^{WT} and $^{-G63S}$ (cre-on and –off) in TSA201 cells

Given the outcomes of the impaired GABA uptake activity of hGAT1^{G63S} in cells, the next step involved the implementation of an *in vivo* tool. Since the *de novo* mutation was found in an individual who presented with parkinsonian symptoms (Leclert *et al.*, 2024), it would be interesting to see how hGAT1^{G63S} manifested in an *in vivo* model. A common gene delivery instrument in neuroscience is the use of AAVs, due to its ability of long-term gene expression within different cell types and animal models (Challis *et al.*, 2022).

For that, hGAT1^{WT} and $^{-G63S}$ had to be subcloned into an AAV-appropriate backbone. The most important structures herein are so-called inverted terminal repeats (ITR), which flank the gene of interest and are crucial for replication and gene packaging into the viral vector (Meier, Fraefel and Seyffert, 2020). Through the cloning process (as described in **3.4 Cloning**), pAAV-DIO-hGAT1^{WT} and $^{-G63S}$ plasmids were successfully produced and confirmed through Sanger sequencing.

Additionally, sequencing results supported different Cre-configurations, namely cre-off and cre-on (**Figure 5 and Figure 8A**) for each plasmid. This is of special interest, given that the Cre-LoxP system is a popular tool for evoking selective gene expression *in vivo* by using cre-on constructs, which is driven through the Cre-recombinase (Nagy, 2000).

In order to investigate these newly cloned constructs, different methods were performed using TSA201 cells. First, to test GAT1 transporter activity, a [^{3}H]-GABA radioligand uptake assay, using the same conditions as before, was conducted. Consistent with hGAT1^{G63S} functionality, pAAV-DIO-hGAT1^{G63S} cre-off confirmed lack of GABA uptake activity, while pAAV-DIO-hGAT1^{WT} afforded specific tiagabine-sensitive [^{3}H]-GABA uptake (**Figure 12A**).

Furthermore, the Cre-dependence of the cre-on configuration for each construct had to be tested for further *in vivo* experiments. TSA201 cells were therefore transiently transfected with a combination of different plasmids (**Figure 9**). Looking at the individually transfected controls, the Cre recombinase as well as hDAT cre-off were strongly expressed (**Figure 15A, Annex**)**.** As expected, pAAV-DIO-hGAT1^{WT} and -^{G63S} cre-off constructs were strongly expressed in a Cre-independent nature (**Figure 12B**)**.** On the other hand, when observing the pAAV-DIO-hGAT1 cre-on plasmids by themselves, the lack of the Cre recombinase led to the G63S variant to not being expressed, whereas WT still appeared to have low expression ability. However, after combining the variants with Cre, signals from both transporter variants were clearly revealed, confirming their Cre-dependence (**Figure 12C**). Similarly, the control hDAT cre-on did not express when transfected by itself, but only in the presence of Cre recombinase (**Figure 15B, Annex**). Through these results, the successful cloning and Cre-dependent expression of the two transporter variants could be confirmed.

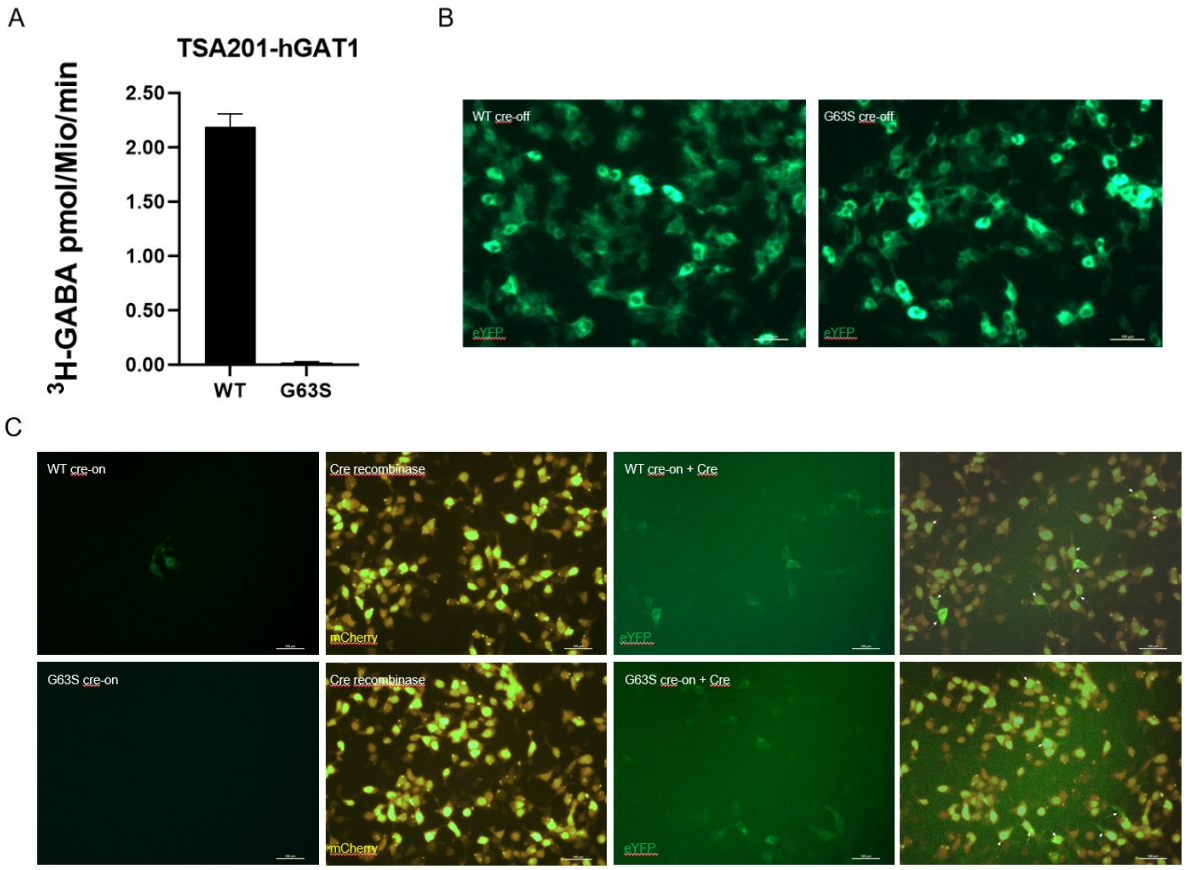

Figure 12 pAAV-DIO-hGAT1^{WT} and $^{-G63S}$ subcloning-success demonstrated by absent [^{3}H]-GABA trafficking in mutant hGAT1 and Cre-dependence in cre-on configurations. (A) *Measurement of [^{3}H]-GABA uptake in TSA201 cells transfected with pAAV-DIO-hGAT1^{WT} or pAAV-DIO-hGAT1^{G63S}. Specific and unspecific uptake were measured with 50 nM [^{3}H]-GABA and presence of 10 µM tiagabine, respectively. n = 1 biological replicate.* ***(B)*** *Representative images of TSA201 cells transfected with pAAV-DIO-hGAT1^{WT} and $^{-G63S}$ cre-off. The eYFP-tagged hGAT1 is shown as a strong, green signal in a Cre-independent configuration.* ***(C)*** *Representative images of TSA201 cells transfected with pAAV-DIO-hGAT1^{WT} or pAAV-DIO-hGAT1^{G63S} in the cre-on configuration. First images of both rows show pAAV-DIO-hGAT1 cre-on without Cre recombinase. The yellow signal represents the mCherry-tagged Cre recombinase, whereas the green signal shows the eYFP-tagged hGAT1. An overlap of both signals displays the co-localization of hGAT1 and TSA201-Cre-mCherry cells, indicated by arrows. Transfection outcomes have been imaged after a 24h incubation.*

4.3 AAV-production in TSA201 cells with pAAV-Syn1-DIO-hDAT (cre-off), pAAV-Syn1-DIO-hGAT1^{WT} and -^{G63S} (cre-on)

Next, I established an AAV production protocol in the Steinkellner lab. AAV generation was initiated in TSA201 cells by using hDAT cre-off as the transporter of choice for testing. Since it was demonstrated that the cre-off configuration works well (see above, **Figure 12B**) and therefore could easily be visualized by fluorescence microscopy (**Figure 15A, Annex**), it made sense to use a control cre-off plasmid to facilitate the tracking of virus production and transduction efficiency.

For AAV generation, viral plasmids were co-transfected with the gene of interest, which take part in delivering various genes helpful for AAV production. Briefly, pAdenoHelper and pAAV-DJ (**Figure 10A and B**) introduced viral-helper factors as well as genes responsible for building the capsid and the replication machinery, respectively (Meier, Fraefel and Seyffert, 2020). Over the course of several days, the spreading of the AAV could be recorded as the signal of the GFP-tagged transporter increased steadily (**Figure 13A**). Successful virus production was tested by transducing TSA201 cells with either extracted virus or virus from the cell culture supernatant and thereafter by investigating cells for eYFP expression (**Figure 13B**).

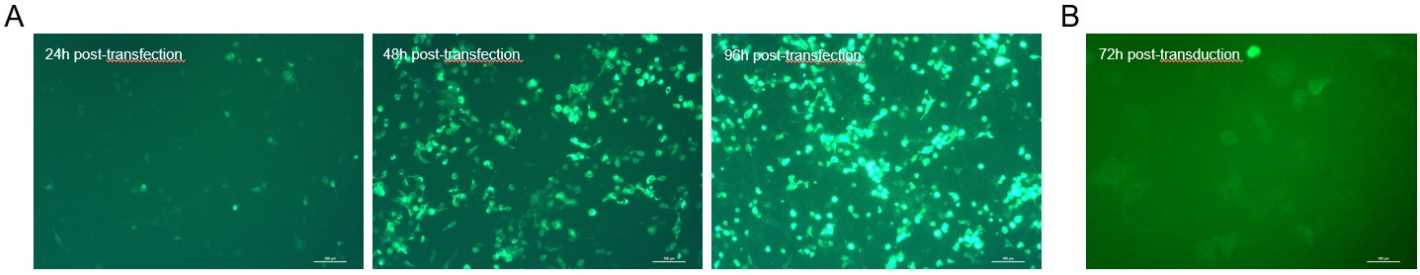

Figure 13 AAV-production with hDAT cre-off showcases successful transduction of TSA201 cells. (A) *Representative images of TSA201 cells transfected with hDAT cre-off. The production timeline exhibits an increasing signal and spreading of the virus within 24h, 48h and 96h post-transfection.* ***(B)*** *Representative image of TSA201 cells transduced with hDAT cre-off virus seen in (A). Transduction outcomes have been seen after incubating the virus for 72h.*

Next, the AAV production process was repeated by using pAAV-DIO-hGAT1^{WT} and pAAV-DIO-hGAT1^{G63S} cre-on plasmids. Since these plasmids are Cre-dependent, the virus spreading could not be tracked directly using fluorescence microscopy since no Cre recombinase is present in these cells. Therefore, for virus testing, an mCherry-tagged Cre recombinase had to be introduced first into TSA201 cells, before transducing them with the viruses. For both variants, transporter expression could be detected in Cre expressing cells (**Figure 14**), but not in cells without Cre-mCherry. When observing the cells after different volumes of the pAAV-DIO-hGAT1^{WT} cre-on virus were added, cells were very susceptible to cell death with increased virus concentrations (**Figure 16, Annex**), suggesting possible toxicity, though this could also be related to Cre expression which is not well tolerated by the cells. Overall, the viruses showed to be functional and effective in an *in vitro* system and have meanwhile also been confirmed *in vivo* by colleagues in the Steinkellner lab.

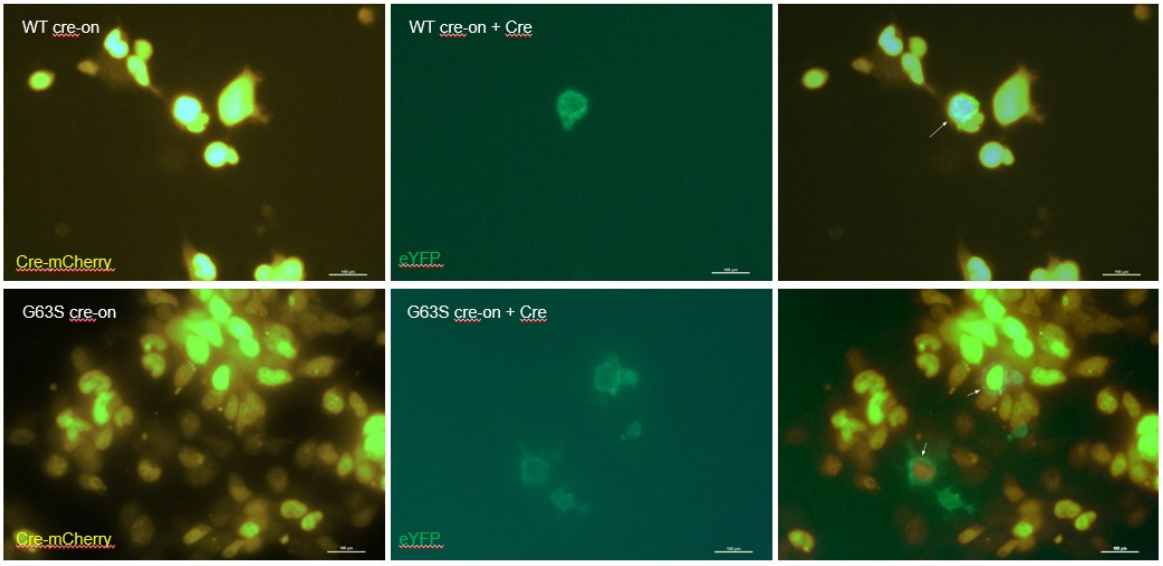

Figure 14 pAAV-DIO-hGAT1^{WT} and $^{-G63S}$ cre-on AAVs are able to transduce TSA201 cells containing Cre recombinase. *Representative images of TSA201-Cre-mCherry cells transduced with pAAV-DIO-hGAT1^{WT} and pAAV-DIO-hGAT1^{G63S} cre-on viruses. The yellow signal represents the mCherry-tagged Cre recombinase, whereas the green signal shows the eYFP-tagged hGAT1. An overlap of both signals displays the co-localization of hGAT1 and TSA201-cre-mCherry cells, indicated by arrows. Transduction outcomes have been seen after incubating the virus for 72h (WT) and 48h (G63S).*

5 Discussion

This project aimed to explore a possible new research perspective related to DA neuron vulnerability and GABA co-release. A hallmark of PD is the selective degeneration of DA neurons within the SNc, where certain cells display a higher resilience, while others are more vulnerable (Surmeier, Obeso and Halliday, 2017). This characteristic was attributed to their heterogeneity as a population, where DA cells have been found to express various markers (Poulin *et al.*, 2020). One of such marker that is co-expressed in DA neurons is GAT1, which has been shown to be crucial for GABA co-release in mice (Tritsch *et al.*, 2014) and has recently also been detected in human midbrain DA neurons (Srinivasan *et al.*, 2025). However, the role of GAT1, in combination with GABA co-release in vulnerability and disease, is still unknown.

Herein, through the discovery of a novel mutation found in GAT1 in a parkinsonian individual with bilateral DA neurodegeneration (Leclert *et al.*, 2024), a possible new factor, that could lead to increased vulnerability, could be explored. Therefore, the GAT1 variant G63S was examined through measuring its [^{3}H]-GABA uptake activity in order to determine transporter functionality and get first insights of its effects *in vitro*. The results showed, that there was a complete abolishment of GABA uptake, which goes hand in hand with a previous report, that explored G63S in the same way (Kanner, 2003). Next, the localization of the mutant was determined in order to ensure, that G63S is the reason why transport activity was lost. It is known for GAT1 variants, that endoplasmic reticulum retention is one of the reasons for reduced GABA uptake (Farhan *et al.*, 2007, 2008; Mermer *et al.*, 2021). Therefore, a trypan blue staining was conducted to visualize the membrane. Indeed, it could be seen that hGAT1^{G63S} was co-localizing with the membrane, indicating that it is transported and expressed on the cell, but dysfunctional.

The position G63 is found in the unwound region of TMD 1 which comprises the ion and substrate binding pocket. Under physiological conditions, G63 was found to be important for upholding internal conformations and is seemingly also involved in interacting with co-transported sodium ions (Skovstrup *et al.*, 2010; Zhu *et al.*, 2023). It could be suggested that the substitution from glycine to serine lead to the

disruption of localized interactions between nearby structures that are similarly responsible for keeping the conformational state intact. This could possibly lead to the disruption of GAT1's possibility to change conformational states overall, since it is also known, that the TMD 1 is involved and rather important when it comes to mediating the shift from outward-open to inward-open states (Krishnamurthy and Gouaux, 2012), therefore losing its ability to transport GABA overall.

In regards to GABA co-release in DA neurons, knock out of GAT1 lead to the loss of co-release ability as well as a disruption in autoregulatory mechanisms of striatal DA neurons (Melani and Tritsch, 2022; Patel *et al.*, 2024). The results obtained from the radioligand uptake assay can be equated to these findings in a sense, that the hGAT1^{G63S} may act like a knockout by having lost its transport function completely.

The next step was to establish a tool that can be used for *in vivo* testing to eventually get more insights into how the variant could possibly impact a model organism and its behavior. In neuroscience, a popular tool to selectively and stably introduce a gene of interest into a brain region are AAVs (Challis *et al.*, 2022). However, for viral vehicles to be able to package a gene, certain structures, namely ITRs, have to be present (Meier, Fraefel and Seyffert, 2020). Accordingly, through classical subcloning, hGAT1^{WT} and hGAT1^{G63S} were respectively subcloned in an AAV-compatible backbone from a preexisting plasmid in the lab (pAAV-hSyn1-DIO). Through Sanger sequencing it was confirmed that positive clones, with cre-on and -off configurations (roughly present at 1:1 ratio), were successfully obtained.

Especially the cre-on configuration is of interest for *in vivo* studies, since it allows one to selectively express the gene of interest in a region where Cre recombinase is exclusively expressed in a specific cell type (Cre-driver line), which is needed for recombining the LoxP sites which govern gene expression (Nagy, 2000). Thus, the clones were tested for their Cre-dependence by either transfecting TSA201 cells with a single plasmid or in combination with a Cre recombinase. As expected, the cre-off configurations were all strongly expressed in the absence of Cre recombinase. In contrast, for the cre-on configurations no signal was seen when transfected by themselves, but only when combined with Cre recombinase. One exception was pAAV-DIO-hGAT1^{WT} cre-on, which was still expressed all by itself, albeit

very weakly. There is no direct explanation as to why this would happen, unless GFP-containing plasmids were unintentionally introduced or the preparation may have been contaminated to some extent with cre-off plasmid. Additionally, the cre-off clones were once again functionally examined through a radioligand uptake assay, which ultimately yielded the same results as before. Together, those outcomes suggest functional plasmids for AAV production, thus *in vivo* application.

Finally, AAVs were produced in such a way, that firstly a control hDAT cre-off plasmid was used. The virus assembly could be tracked easily, which could be seen through steadily increasing signals day by day. Once the virus was extracted and tested, which lead to successfully transduced cells, the protocol was seen convincing enough to start the AAV assembly with the hGAT1 cre-on constructs. However, certain problems emerged which impeded the production process. TSA201 cells had to be transfected first with a Cre recombinase in order for the cre-on constructs to be visible. Once the extracted viruses were introduced to the Cre-containing cells, a lot of cell death has been noticed, especially with increasing concentrations of the virus. This has not been seen before with any cre-off virus which was tested on cells, which made the discovery rather surprising and suggests substantial toxicity coming from Cre expression. Even with further adaptations of the protocol to ensure that the final virus solution was as clean as possible, no improvement has been made. Additionally, fewer cells were seen to express the cre-on constructs in comparison to the cre-off ones. It has been observed in the past in the Steinkellner lab, that cells that were transfected with the Cre recombinase did not do well, indicating that the main problem could indeed be the introduction of the Cre recombinase to the cells. Nevertheless, the AAV production and extraction still showed promising results with the cre-off constructs. Still, introducing a more thorough extraction method which purifies the final virus solution might be an adaptation worth making.

Through the obtained *in vitro* data on hGAT1^{G63S} transport function, first insights were made about a novel mutation which may have implications in DA vulnerability. The next step would be to introduce the variant into an *in vivo* model to have a better understanding of the mutant's impact on possible behavioral changes, thus eventual disease development and progression. Additionally, cell-type specific assays could be performed to expand the *in vivo* investigations of the dysfunctional transporter.

Nevertheless, through studying the fundamental involvement of co-release and the role of GAT1 in maintaining GABA homeostasis, a novel view on certain aspects of PD could be obtained - a disease, which still has no cure. Altogether, those specific reasons underscore the need for further exploration of an aspiring and promising topic, in hopes of eventually finding a starting point for future disease-alleviating therapies.

List of References

Armstrong, M. J. and Okun, M. S. (2020) 'Diagnosis and Treatment of Parkinson Disease: A Review', *JAMA - Journal of the American Medical Association*, 323(6), pp. 548–560. doi: 10.1001/jama.2019.22360.

Baglo, Y. *et al.* (2013) 'Homology Modeling of Human γ-Butyric Acid Transporters and the Binding of Pro-Drugs 5-Aminolevulinic Acid and Methyl Aminolevulinic Acid Used in Photodynamic Therapy', *PLoS ONE*, 8(6). doi: 10.1371/journal.pone.0065200.

Bak, L. K., Schousboe, A. and Waagepetersen, H. S. (2006) 'The glutamate / GABA-glutamine cycle : aspects of transport , neurotransmitter homeostasis and ammonia transfer', pp. 641–653. doi: 10.1111/j.1471-4159.2006.03913.x.

Bandopadhyay, R. *et al.* (2022) 'Molecular Mechanisms and Therapeutic Strategies for Levodopa-Induced Dyskinesia in Parkinson's Disease: A Perspective Through Preclinical and Clinical Evidence', *Frontiers in Pharmacology*, 13(April), pp. 1–23. doi: 10.3389/fphar.2022.805388.

Barcomb, K. and Ford, C. P. (2023) 'Alterations in neurotransmitter co-release in Parkinson ' s disease', *Experimental Neurology*, 370(September), p. 114562. doi: 10.1016/j.expneurol.2023.114562.

Beach, T. G. *et al.* (2010) 'Multi-organ distribution of phosphorylated α-synuclein histopathology in subjects with Lewy body disorders', *Acta Neuropathologica*, 119(6), pp. 689–702. doi: 10.1007/s00401-010-0664-3.

Beaulieu, J. and Gainetdinov, R. R. (2011) 'The Physiology , Signaling , and Pharmacology of Dopamine Receptors', 63(1), pp. 182–217. doi: 10.1124/pr.110.002642.182.

Bender, A. *et al.* (2006) 'High levels of mitochondrial DNA deletions in substantia nigra neurons in aging and Parkinson disease', *Nature Genetics*, 38(5), pp. 515–517. doi: 10.1038/ng1769.

Bodea, G. O. and Blaess, S. (2015) 'Establishing diversity in the dopaminergic

system', *FEBS Lett*, 589, pp. 3773–3785. doi: 10.1016/j.febslet.2015.09.016.

Braak, H. *et al.* (2003) 'Staging of brain pathology related to sporadic Parkinson's disease', *Neurobiology of Aging*, 24(2), pp. 197–211. doi: 10.1016/S0197-4580(02)00065-9.

Braak, H. *et al.* (2004) 'Stages in the development of Parkinson's disease-related pathology', *Cell and Tissue Research*, 318(1), pp. 121–134. doi: 10.1007/s00441-004-0956-9.

Brodacki, B. *et al.* (2008) 'Serum interleukin (IL-2, IL-10, IL-6, IL-4), TNFα, and INFγ concentrations are elevated in patients with atypical and idiopathic parkinsonism', *Neuroscience Letters*, 441(2), pp. 158–162. doi: 10.1016/j.neulet.2008.06.040.

Brolin, K. A. *et al.* (2025) 'Environmental Risk Factors for Parkinson ' s Disease : A Critical Review and Policy Implications', 40(2), pp. 204–221. doi: 10.1002/mds.30067.

Burré, J., Sharma, M. and Südhof, T. C. (2018) 'Cell biology and pathophysiology of α-synuclein', *Cold Spring Harbor Perspectives in Medicine*, 8(3). doi: 10.1101/cshperspect.a024091.

Cai, Y. and Ford, C. P. (2018) 'Dopamine Cells Differentially Regulate Striatal Cholinergic Transmission across Regions through Corelease of Dopamine and Glutamate Article Dopamine Cells Differentially Regulate Striatal Cholinergic Transmission across Regions through Corelease of Dopamine and Glutamate', *CellReports*, 25(11), pp. 3148-3157.e3. doi: 10.1016/j.celrep.2018.11.053.

Calabresi, P. *et al.* (2014) 'Direct and indirect pathways of basal ganglia: A critical reappraisal', *Nature Neuroscience*, 17(8), pp. 1022–1030. doi: 10.1038/nn.3743.

Cersosimo, M. G. and Benarroch, E. E. (2012) 'Autonomic involvement in Parkinson's disease: Pathology, pathophysiology, clinical features and possible peripheral biomarkers', *Journal of the Neurological Sciences*, 313(1–2), pp. 57–63. doi: 10.1016/j.jns.2011.09.030.

Challis, R. C. *et al.* (2022) 'Adeno-Associated Virus Toolkit to Target Diverse Brain Cells', pp. 447–469.

Chen, N.-H., Reith, M. E. A. and Quick, M. W. (2004) ‘Synaptic uptake and beyond : the sodium- and chloride-dependent neurotransmitter transporter family SLC6’, 1, pp. 519–531. doi: 10.1007/s00424-003-1064-5.

Chen, Y. *et al.* (2021) ‘Non-Genetic Risk Factors for Parkinson ’ s Disease : An Overview of 46 Systematic Reviews’, 11, pp. 919–935. doi: 10.3233/JPD-202521.

Conrad, W. S. *et al.* (2024) ‘Proportion and distribution of neurotransmitter-defined cell types in the ventral tegmental area and substantia nigra pars compacta’, *Addiction Neuroscience*, 13(October), p. 100183. doi: 10.1016/j.addicn.2024.100183.

Desplats, P. *et al.* (2009) ‘Inclusion formation and neuronal cell death through neuron-to-neuron transmission of α-synuclein’, *Proceedings of the National Academy of Sciences of the United States of America*, 106(31), pp. 13010–13015. doi: 10.1073/pnas.0903691106.

Devi, L. *et al.* (2008) ‘Mitochondrial import and accumulation of α-synuclein impair complex I in human dopaminergic neuronal cultures and Parkinson disease brain’, *Journal of Biological Chemistry*, 283(14), pp. 9089–9100. doi: 10.1074/jbc.M710012200.

Dorsey, E. R. and Bloem, B. R. (2018) ‘The Parkinson pandemic - A call to action’, *JAMA Neurology*, 75(1), pp. 9–10. doi: 10.1001/jamaneurol.2017.3299.

Dunkerley, K. M. *et al.* (2022) ‘Distinct phosphorylation signals drive acceptor versus free ubiquitin chain targeting by parkin’, *Biochemical Journal*, 479(6), pp. 751–766. doi: 10.1042/BCJ20210741.

Eiden, L. E. and Schäfer, M. K. (2004) ‘The vesicular amine transporter family (SLC18): amine / proton antiporters required for vesicular accumulation and regulated exocytotic secretion of monoamines and acetylcholine’, pp. 636–640. doi: 10.1007/s00424-003-1100-5.

Elstner, M. *et al.* (2011) ‘Expression analysis of dopaminergic neurons in Parkinson’s disease and aging links transcriptional dysregulation of energy metabolism to cell death’, *Acta Neuropathol*. doi: 10.1007/s00401-011-0828-9.

Farhan, H. *et al.* (2007) ‘Concentrative Export from the Endoplasmic Reticulum of the y-Aminobutyric Acid Transporter 1 Requires Binding to SEC24D’, *The Journal of Biological Chemistry*, 282(10), pp. 7679–7689. doi: 10.1074/jbc.M609720200.

Farhan, H. *et al.* (2008) ‘Signal-dependent export of GABA transporter 1 from the ER-Golgi intermediate compartment is specified by a C-terminal motif’, *Journal of Cell Science*. doi: 10.1242/jcs.017681.

Floresco, S. B. *et al.* (2003) ‘Afferent modulation of dopamine neuron firing differentially regulates tonic and phasic dopamine transmission’, 6(9), pp. 968–973. doi: 10.1038/nn1103.

Focke, P. J., Wang, X. and Larsson, H. P. (2013) ‘Review Neurotransmitter Transporters : Structure Meets Function’, *Structure/Folding and Design*, 21(5), pp. 694–705. doi: 10.1016/j.str.2013.03.002.

Fortin, G. M. *et al.* (2012) ‘Glutamate Corelease Promotes Growth and Survival of Midbrain Dopamine Neurons’, 32(48), pp. 17477–17491. doi: 10.1523/JNEUROSCI.1939-12.2012.

Furukawa, K. *et al.* (2022) ‘Motor Progression and Nigrostriatal Neurodegeneration in Parkinson Disease’, *Annals of Neurology*, 92(1), pp. 110–121. doi: 10.1002/ana.26373.

Fushiki, A. *et al.* (2024) ‘A Vulnerable Subtype of Dopaminergic Neurons Drives Early Motor Deficits in Parkinson ’ s Disease’.

Gassmann, M. and Bettler, B. (2012) ‘Regulation of neuronal GABA B receptor functions by subunit composition’, 13(June). doi: 10.1038/nrn3249.

Gelders, G., Baekelandt, V. and Van der Perren, A. (2018) ‘Linking neuroinflammation and neurodegeneration in parkinson’s disease’, *Journal of Immunology Research*, 2018. doi: 10.1155/2018/4784268.

Gelpi, E. *et al.* (2014) ‘Multiple organ involvement by alpha-synuclein pathology in lewy body disorders’, *Movement Disorders*, 29(8), pp. 1010–1018. doi: 10.1002/mds.25776.

Gerfen, C. R. and Surmeier, D. J. (2011) ‘Modulation of striatal projection systems by dopamine’, *Annual Review of Neuroscience*, 34, pp. 441–466. doi: 10.1146/annurev-neuro-061010-113641.

Goodspeed, K. *et al.* (2020) ‘Current knowledge of SLC6A1-related neurodevelopmental disorders’, *Brain Communications*, 2(2), pp. 1–10. doi: 10.1093/braincomms/fcaa170.

Hinkle, J. T. *et al.* (2022) ‘STING mediates neurodegeneration and neuroinflammation in nigrostriatal α-synucleinopathy’, *Proceedings of the National Academy of Sciences of the United States of America*, 119(15), pp. 1–8. doi: 10.1073/pnas.2118819119.

Hnasko, T. S. *et al.* (2010) ‘Vesicular Glutamate Transport Promotes Dopamine Storage and Glutamate Corelease In Vivo’, *Neuron*, 65(5), pp. 643–656. doi: 10.1016/j.neuron.2010.02.012.

Huang, E. J. (2015) ‘Ventral midbrain dopaminergic neurons: From neurogenesis to neurodegeneration’, *FEBS Lett*, 589, pp. 3691–3692. doi: 10.1016/j.febslet.2015.11.008.

Hunot, S. *et al.* (1999) ‘FcεRII/CD23 is expressed in Parkinson’s disease and induces, in vitro, production of nitric oxide and tumor necrosis factor-α in glial cells’, *Journal of Neuroscience*, 19(9), pp. 3440–3447. doi: 10.1523/jneurosci.19-09-03440.1999.

Hyland, B. I. *et al.* (2002) ‘FIRING MODES OF MIDBRAIN DOPAMINE CELLS IN THE FREELY MOVING RAT’, 114(2).

Juge, N. *et al.* (2009) ‘Vesicular Inhibitory Amino Acid Transporter Is a $Cl_{\mathcal{U}}$ /γ-Aminobutyrate Co-transporter’, *Journal of Biological Chemistry*, 284(50), pp. 35073–35078. doi: 10.1074/jbc.M109.062414.

Kamath, T. *et al.* (2022) *Single-cell genomic profiling of human dopamine neurons identifies a population that selectively degenerates in Parkinson’s disease*. Springer US. doi: 10.1038/s41593-022-01061-1.

Kane, L. A. *et al.* (2014) ‘PINK1 phosphorylates ubiquitin to activate parkin E3

ubiquitin ligase activity', *Journal of Cell Biology*, 205(2), pp. 143–153. doi: 10.1083/jcb.201402104.

Kanner, B. I. (2003) 'Transmembrane domain I of the γ-aminobutyric acid transporter GAT-1 plays a crucial role in the transition between cation leak and transport modes', *Journal of Biological Chemistry*, 278(6), pp. 3705–3712. doi: 10.1074/jbc.M210525200.

Keeney, P. M. *et al.* (2006) 'Parkinson's disease brain mitochondrial complex I has oxidatively damaged subunits and is functionally impaired and misassembled', *Journal of Neuroscience*, 26(19), pp. 5256–5264. doi: 10.1523/JNEUROSCI.0984-06.2006.

Kim, H. *et al.* (2023) 'GABAergic-like dopamine synapses in the brain', *CellReports*, 42(10), p. 113239. doi: 10.1016/j.celrep.2023.113239.

Kim, J. I. *et al.* (2015) 'Aldehyde dehydrogenase 1a1 mediates a GABA synthesis pathway in midbrain dopaminergic neurons', *Science*, 350(6256), pp. 102–106. doi: 10.1126/science.aac4690.

Kitada, T. *et al.* (1998) 'Mutations in the parkin gene cause autosomal recessive juvenile parkinsonism', 169(1993), pp. 166–169.

Klein, C. and Westenberger, A. (2012) 'Genetics of Parkinson's disease'. doi: 10.1016/B978-044452809-4/50169-1.

Klein, M. O. *et al.* (2019) 'Dopamine : Functions , Signaling , and Association with Neurological Diseases', *Cellular and Molecular Neurobiology*, 39(1), pp. 31–59. doi: 10.1007/s10571-018-0632-3.

Koeglsperger, T. *et al.* (2023) 'Neuropathology of incidental Lewy body & prodromal Parkinson ' s disease', pp. 1–18. doi: 10.1186/s13024-023-00622-7.

Koopman, W. J. *et al.* (2012) 'OXPHOS mutations and neurodegeneration', *The EMBO Journal*, 32, pp. 9–29. doi: 10.1038/emboj.2012.300.

Krishnamurthy, H. and Gouaux, E. (2012) 'X-ray structures of LeuT in substrate-free outward-open and apo inward-open states', *Nature*, 25. doi: 10.1038/nature10737.

Kristensen, A. S. *et al.* (2011) ‘SLC6 neurotransmitter transporters: Structure, function, and regulation’, *Pharmacological Reviews*, 63(3), pp. 585–640. doi: 10.1124/pr.108.000869.

Kutik, S. *et al.* (2007) ‘Cooperation of translocase complexes in mitochondrial protein import’, *Journal of Cell Biology*, 179(4), pp. 585–591. doi: 10.1083/jcb.200708199.

Lanciego, J. L., Luquin, N. and Obeso, J. A. (2012) ‘Functional neuroanatomy of the basal ganglia’, *Cold Spring Harbor Perspectives in Medicine*, 2(12). doi: 10.1101/cshperspect.a009621.

Langston, J. W. (2017) ‘The MPTP Story’, 7, pp. 11–19. doi: 10.3233/JPD-179006.

Lazarou, M. *et al.* (2015) ‘The ubiquitin kinase PINK1 recruits autophagy receptors to induce mitophagy’, *Nature*, 524(7565), pp. 309–314. doi: 10.1038/nature14893.

Leclert, V. *et al.* (2024) ‘ Globus Pallidus Lesion With Iron Deposition and Dopaminergic Denervation in a Patient With a Pathogenic SLC6A1 Variant ’, *Neurology Genetics*, 10(2), pp. 1–5. doi: 10.1212/nxg.0000000000200136.

Loo, D. D. F. *et al.* (2000) ‘Role of Cl - in Electrogenic Na + -coupled Cotransporters GAT1 and SGLT’, *Journal of Biological Chemistry*, 275(48), pp. 37414–37422. doi: 10.1074/jbc.M007241200.

Lopes, X. E. F. *et al.* (2019) ‘Inhibition of Nigrostriatal Dopamine Release by Striatal GABA A and GABA B Receptors’, 39(6), pp. 1058–1065.

Lu, C. and Hilgemann, D. W. (1999) ‘GAT1 (GABA : Na + : Cl -) Cotransport Function - Kinetic Studies in Giant Xenopus Oocyte Membrane Patches’, 114(September).

Luk, K. C. *et al.* (2012) ‘Intracerebral inoculation of pathological α-synuclein initiates a rapidly progressive neurodegenerative α-synucleinopathy in mice’, *Journal of Experimental Medicine*, 209(5), pp. 975–988. doi: 10.1084/jem.20112457.

Luppi, M. P. *et al.* (2021) ‘Sox6 expression distinguishes dorsally and ventrally biased dopamine neurons in the substantia nigra with distinctive properties and

embryonic origins', *cell reports*. doi: 10.1016/j.celrep.2021.109975.

Mahul-Mellier, A.-L. *et al.* (2020) 'The process of Lewy body formation, rather than simply α-synuclein fibrillization, is one of the major drivers of neurodegeneration', *PNAS*. doi: 10.6084/m9.figshare.11842389.v2.

Meier, A. F., Fraefel, C. and Seyffert, M. (2020) 'The Interplay between Adeno-Associated Virus and Its Helper Viruses', *Viruses*, pp. 8–12.

Meiser, J., Weindl, D. and Hiller, K. (2013) 'Complexity of dopamine metabolism', pp. 1–18.

Melani, R. and Tritsch, N. X. (2022) 'Inhibitory co-transmission from midbrain dopamine neurons relies on presynaptic GABA uptake', *Cell Reports*, 39(3), p. 110716. doi: 10.1016/j.celrep.2022.110716.

Mermer, F. *et al.* (2021) 'Common molecular mechanisms of SLC6A1 variant-mediated neurodevelopmental disorders in astrocytes and neurons', *Brain*, 144(8), pp. 2499–2512. doi: 10.1093/brain/awab207.

Morais, V. A. *et al.* (2009) 'Parkinson's disease mutations in PINK1 result in decreased Complex I activity and deficient synaptic function', *EMBO Molecular Medicine*, 1(2), pp. 99–111. doi: 10.1002/emmm.200900006.

Motiwala, Z. *et al.* (2022) 'Structural basis of GABA reuptake inhibition', *Nature*, 606(7915), pp. 820–826. doi: 10.1038/s41586-022-04814-x.

Nagy, A. (2000) 'Cre Recombinase : The Universal Reagent for Genome Tailoring', 109, pp. 99–109.

Narendra, D. P. *et al.* (2010) 'PINK1 is selectively stabilized on impaired mitochondria to activate Parkin', *PLoS Biology*, 8(1). doi: 10.1371/journal.pbio.1000298.

Olanow, C. W. and Stocchi, F. (2018) 'Levodopa: A new look at an old friend', *Movement Disorders*, 33(6), pp. 859–866. doi: 10.1002/mds.27216.

Omote, H. and Moriyama, Y. (2025) 'Vesicular Neurotransmitter Transporters : An Approach for Studying Transporters With Purified Proteins', pp. 39–50. doi:

10.1152/physiol.00033.2012.

Ovallath, S. and Sulthana, B. (2017) ‘Levodopa: History and therapeutic applications’, *Annals of Indian Academy of Neurology*, 20(3), p. 185. doi: 10.4103/aian.AIAN_241_17.

Özçete, Ö. D., Banerjee, A. and Kaeser, P. S. (2024) ‘Mechanisms of neuromodulatory volume transmission’, *Molecular Psychiatry*, (May). doi: 10.1038/s41380-024-02608-3.

Patel, J. C. *et al.* (2024) ‘GABA co-released from striatal dopamine axons dampens phasic dopamine release through autoregulatory GABA A receptors’, *CellReports*, 43(3), p. 113834. doi: 10.1016/j.celrep.2024.113834.

Pickles, S., Vigié, P. and Youle, R. J. (2018) ‘Mitophagy and Quality Control Mechanisms in Mitochondrial Maintenance’, *Current Biology*, 28(4), pp. R170–R185. doi: 10.1016/j.cub.2018.01.004.

Poewe, W. *et al.* (2017) ‘Parkinson disease’, *Nature Reviews Disease Primers*, 3, pp. 1–21. doi: 10.1038/nrdp.2017.13.

Poewe, W. *et al.* (2020) ‘New hopes for disease modification in Parkinson’s Disease’, *Neuropharmacology*, 171(January), p. 108085. doi: 10.1016/j.neuropharm.2020.108085.

Polymeropoulos, M. H. *et al.* (1997) ‘Mutation in the α -Synuclein Gene Identified in Families with Parkinson ’ s Disease Mutation in the ␣ -Synuclein Gene Identified in Families with Parkinson ’ s Disease’, 2045(1997). doi: 10.1126/science.276.5321.2045.

Poulin, J. *et al.* (2014) ‘Defining Midbrain Dopaminergic Neuron Diversity by Article Defining Midbrain Dopaminergic Neuron Diversity by Single-Cell Gene Expression Profiling’, *CellReports*, 9(3), pp. 930–943. doi: 10.1016/j.celrep.2014.10.008.

Poulin, J. *et al.* (2018) ‘Mapping projections of molecularly defined dopamine neuron subtypes using intersectional genetic approaches’, *Nature Neuroscience*, 21(September). doi: 10.1038/s41593-018-0203-4.

Poulin, J. F. *et al.* (2020) ‘Classification of Midbrain Dopamine Neurons Using Single-Cell Gene Expression Profiling Approaches’, *Trends in Neurosciences*, 43(3), pp. 155–169. doi: 10.1016/j.tins.2020.01.004.

Pringsheim, T. *et al.* (2014) ‘The prevalence of Parkinson’s disease: A systematic review and meta-analysis’, *Movement Disorders*, 29(13), pp. 1583–1590. doi: 10.1002/mds.25945.

Protasoni, M. and Zeviani, M. (2021a) ‘Mitochondrial Structure and Bioenergetics in Normal and Disease Conditions’, *Molecular Sciences*. doi: 10.3390/ijms.

Protasoni, M. and Zeviani, M. (2021b) ‘Molecular Sciences Mitochondrial Structure and Bioenergetics in Normal and Disease Conditions’, *In. J. Mol. Sci*, 22(2). Available at: https://doi.org/10.3390/ijms.

Quinn, P. M. J. *et al.* (2020) ‘PINK1/PARKIN signalling in neurodegeneration and neuroinflammation’, *Acta neuropathologica communications*, 8(1), p. 189. doi: 10.1186/s40478-020-01062-w.

Rango, M., Bonifati, C. and Bresolin, N. (2006) ‘Parkinson’s disease and brain mitochondrial dysfunction: a functional phosphorus magnetic resonance spectroscopy study’, *Journal of Cerebral Blood Flow & Metabolism*, 26, pp. 283–290. doi: 10.1038/sj.jcbfm.9600192.

Riederer, P. *et al.* (2025) *Levodopa treatment: impacts and mechanisms throughout Parkinson’s disease progression*, *Journal of Neural Transmission*. Springer Vienna. doi: 10.1007/s00702-025-02893-4.

Roth, F. C. and Draguhn, A. (2012) ‘GABA metabolism and transport: Effects on synaptic efficacy’, *Neural Plasticity*. doi: 10.1155/2012/805830.

Sanyal, J. *et al.* (2010) ‘Environmental and Familial Risk Factors of Parkinsons Disease : Case-Control Study’, pp. 637–642.

Schapira, A. H. V., Chaudhuri, K. R. and Jenner, P. (2017) ‘Non-motor features of Parkinson disease’, *Nature Reviews Neuroscience*, 18(7), pp. 435–450. doi: 10.1038/nrn.2017.62.

Scimemi, A. (2014) ‘Structure, function, and plasticity of GABA transporters’, *Frontiers in Cellular Neuroscience*, 8(JUN), pp. 1–14. doi: 10.3389/fncel.2014.00161.

Shah, N. *et al.* (2024) ‘A transporter’s doom or destiny: SLC6A1 in health and disease, novel molecular targets and emerging therapeutic prospects’, *Frontiers in Molecular Neuroscience*, 17(August), pp. 1–11. doi: 10.3389/fnmol.2024.1466694.

Shahmoradian, S. H. *et al.* (2019) ‘Lewy pathology in Parkinson’s disease consists of crowded organelles and lipid membranes’, *Nature Neuroscience*, 22(7), pp. 1099–1109. doi: 10.1038/s41593-019-0423-2.

Shiba-Fukushima, K. *et al.* (2012) ‘PINK1-mediated phosphorylation of the Parkin ubiquitin-like domain primes mitochondrial translocation of Parkin and regulates mitophagy’, *Scientific Reports*, 2, pp. 1–8. doi: 10.1038/srep01002.

Shimoji, M. *et al.* (2009) ‘CXCR4 and CXCL12 expression is increased in the nigro-striatal system of Parkinson’s disease’, *Neurotoxicity Research*, 16(3), pp. 318–328. doi: 10.1007/s12640-009-9076-3.

Sigel, E. and Steinmann, M. E. (2012) ‘Structure , Function , and Modulation of GABAA receptors’, 287(48), pp. 40224–40231. doi: 10.1074/jbc.R112.386664.

Skovstrup, S. *et al.* (2010) ‘Homology modelling of the GABA transporter and analysis of tiagabine binding’, *ChemMedChem*, 5(7), pp. 986–1000. doi: 10.1002/cmdc.201000100.

Smajic, S. *et al.* (2022) ‘Single-cell sequencing of human midbrain reveals glial activation and a Parkinson-specific neuronal state’, *Brain*, 145(3), pp. 964–978. doi: 10.1093/brain/awab446.

Sochocka, M., Satler Diniz, B. and Leszek, J. (2017) ‘Inflammatory Response in the CNS: Friend or Foe?’, *Molecular Neurobiology*. doi: 10.1007/s12035-016-0297-1.

Spillantini, M. G. *et al.* (1998) ‘α-Synuclein in filamentous inclusions of Lewy bodies from Parkinson’s disease and dementia with Lewy bodies’, *Proceedings of the National Academy of Sciences of the United States of America*, 95(11), pp. 6469–6473. doi: 10.1073/pnas.95.11.6469.

Sprenger, F. S. *et al.* (2015) ‘Enteric nervous system a-synuclein immunoreactivity in idiopathic REM sleep behavior disorder’, *Neurology*, 85(20), pp. 1761–1768. doi: 10.1212/WNL.0000000000002126.

Srinivasan, S. *et al.* (2025) ‘Evidence for low affinity of GABA at the vesicular monoamine transporter VMAT2- Implications for transmitter co-release from dopamine neurons’, *Neuropharmacology*, 270(February). Available at: https://doi.org/10.1101/2024.07.04.602053.

Steinkellner, T. *et al.* (2018) ‘Role for VGLUT2 in selective vulnerability of midbrain dopamine neurons’, *Journal of Clinical Investigation*, 128(2), pp. 774–788. doi: 10.1172/JCI95795.

Steinkellner, T. *et al.* (2022) ‘Dopamine neurons exhibit emergent glutamatergic identity in Parkinson’s disease’, *Brain*, 145(3), pp. 879–886. doi: 10.1093/brain/awab373.

Stensrud, M. J., Purchades, M. and Gundersen, V. (2014) ‘GABA is localized in dopaminergic synaptic vesicles in the rodent striatum’, 3, pp. 1901–1912. doi: 10.1007/s00429-013-0609-4.

Sulzer, D. and Rayport, S. (2000) ‘Dale ’ s principle and glutamate corelease from ventral midbrain dopamine neurons Review Article’, pp. 45–52.

Surmeier, D. J. (2018) ‘Determinants of dopaminergic neuron loss in Parkinson’s disease’, *FEBS Journal*, 285(19), pp. 3657–3668. doi: 10.1111/febs.14607.

Surmeier, D. J., Obeso, J. A. and Halliday, G. M. (2017) ‘Selective neuronal vulnerability in Parkinson disease’, *Nature reviews*. doi: 10.1038/nrn.2016.178.

Tekin, I. *et al.* (2014) *Complex molecular regulation of tyrosine hydroxylase*. doi: 10.1007/s00702-014-1238-7.

Tolosa, E. *et al.* (2021) ‘Challenges in the diagnosis of Parkinson’s disease’, *The Lancet Neurology*, 20(5), pp. 385–397. doi: 10.1016/S1474-4422(21)00030-2.

Tritsch, N. X. *et al.* (2014) ‘Midbrain dopamine neurons sustain inhibitory transmission using plasma membrane uptake of GABA, not synthesis’, *eLife*,

2014(3), pp. 1–20. doi: 10.7554/eLife.01936.

Tritsch, N. X., Ding, J. B. and Sabatini, B. L. (2012) 'Dopaminergic neurons inhibit striatal output through non-canonical release of GABA', *Nature*, 490(7419), pp. 262–266. doi: 10.1038/nature11466.

Tritsch, N. X., Granger, A. J. and Sabatini, B. L. (2016) 'Mechanisms and functions of GABA co - release', *Nature Reviews Neuroscience*. doi: 10.1038/nrn.2015.21.

Tysnes, O. B. and Storstein, A. (2017) 'Epidemiology of Parkinson's disease', *Journal of Neural Transmission*, 124(8), pp. 901–905. doi: 10.1007/s00702-017-1686-y.

Umek, N. *et al.* (2018) 'Dopamine Autoxidation Is Controlled by Acidic pH', 11(December), pp. 1–8. doi: 10.3389/fnmol.2018.00467.

Vaaga, C. E., Borisovska, M. and Westbrook, G. L. (2014) 'Dual-transmitter neurons : functional implications of co-release and co-transmission', *Current Opinion in Neurobiology*, 29, pp. 25–32. doi: 10.1016/j.conb.2014.04.010.

Valente, E. M. *et al.* (2001) 'Localization of a Novel Locus for Autosomal Recessive Early-Onset Parkinsonism , PARK6 , on Human Chromosome 1p35-p36', pp. 895–900.

Vascellari, S. and Manzin, A. (2021) 'Parkinson's Disease: A Prionopathy?' Available at: https://doi.org/10.3390/ijms22158022.

Vekrellis, K., Rideout, H. J. and Stefanis, L. (2004) 'Neurobiology of α-synuclein', *Molecular Neurobiology*, 30(1), pp. 1–21. doi: 10.1385/mn:30:1:001.

Volpicelli-Daley, L. A. *et al.* (2011) 'Exogenous α-Synuclein Fibrils Induce Lewy Body Pathology Leading to Synaptic Dysfunction and Neuron Death', *Neuron*, 72(1), pp. 57–71. doi: 10.1016/j.neuron.2011.08.033.

Warren Olanow, C. *et al.* (2013) 'Factors predictive of the development of Levodopa-induced dyskinesia and wearing-off in Parkinson's disease', *Movement Disorders*, 28(8), pp. 1064–1071. doi: 10.1002/mds.25364.

Yamashita, A. *et al.* (2005) 'Crystal structure of a bacterial homologue of Na+/Cl --

dependent neurotransmitter transporters', *Nature*, 437(7056), pp. 215–223. doi: 10.1038/nature03978.

Ye, J. *et al.* (2025) 'Molecular basis of vesicular monoamine transport and neurological drug interactions'. doi: 10.1016/j.celrep.2025.116490.

Zafar, S. and Jabeen, I. (2018) 'Structure , Function , and Modulation of γ - Aminobutyric Acid Transporter 1 (GAT1) in Neurological Disorders : A Pharmacoinformatic Prospective', 6(September), pp. 1–19. doi: 10.3389/fchem.2018.00397.

Zhang, Q. *et al.* (2024) 'Insights and progress on the biosynthesis , metabolism , and physiological functions of gamma-aminobutyric acid (GABA): a review', pp. 1–34. doi: 10.7717/peerj.18712.

Zhao, N. *et al.* (2021) 'Quality of life in Parkinson's disease: A systematic review and meta-analysis of comparative studies', *CNS Neuroscience and Therapeutics*, 27(3), pp. 270–279. doi: 10.1111/cns.13549.

Zheng, G., Dwoskin, L. P. and Crooks, P. A. (2006) 'Vesicular Monoamine Transporter 2 : Role as a Novel Target for Drug Development', 8(4), pp. 682–692.

Zhu, A. *et al.* (2023) 'Molecular basis for substrate recognition and transport of human GABA transporter GAT1', *Nature Structural and Molecular Biology*, 30(7), pp. 1012–1022. doi: 10.1038/s41594-023-00983-z.

Zimprich, A. *et al.* (2004) 'Mutations in LRRK2 Cause Autosomal-Dominant Parkinsonism with Pleomorphic Pathology', 44, pp. 601–607.

Annex

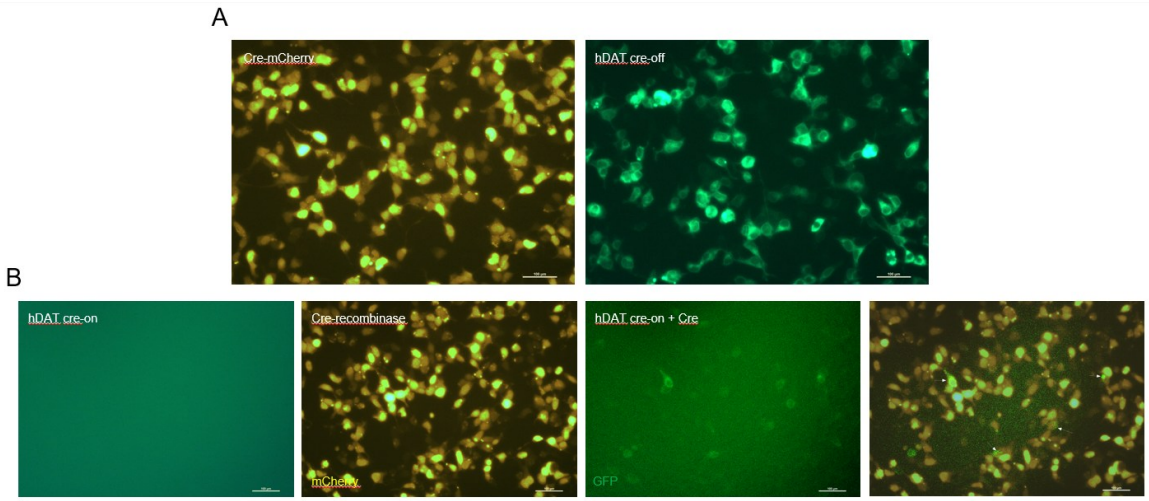

Figure 15 Controls for Cre-configuration testing. (A) *Representative images of TSA201 cells transfected with either Cre-mCherry (yellow) or hDAT cre-off (green).* ***(B)*** *Representative images of TSA201 cells transfected with hDAT in the cre-on configuration. First image shows hDAT cre-on without Cre recombinase co-transfection. The yellow signal represents the mCherry-tagged Cre recombinase, whereas the green signal shows the GFP-tagged hDAT. An overlap of both signals displays the co-localization of hDAT and TSA201-cre-mCherry cells, indicated by arrows. Transfection outcomes have been imaged after a 24h incubation.*

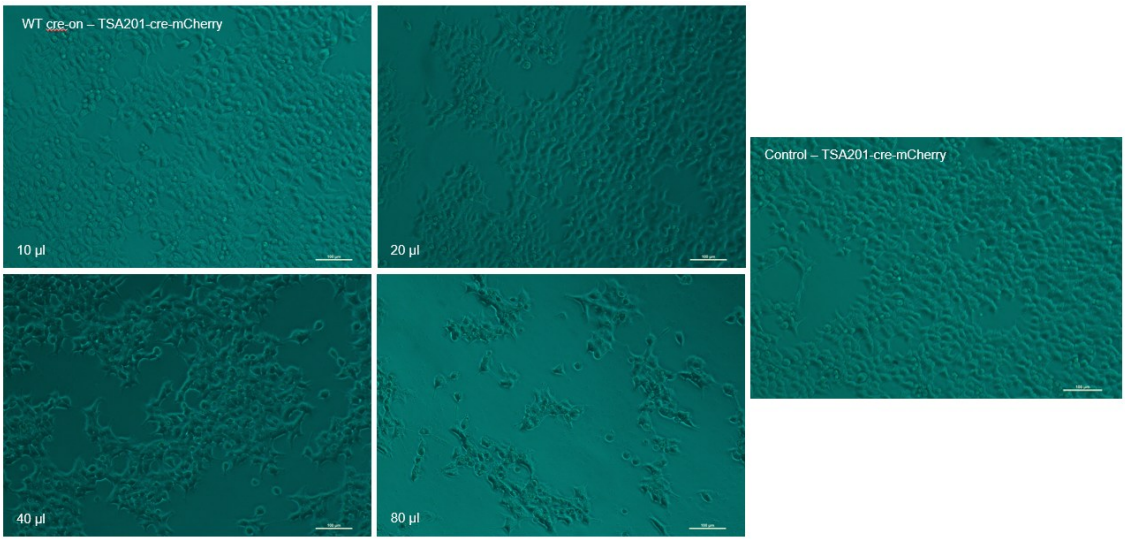

Figure 16 TSA201-Cre-mCherry cells susceptible to cell death with increased concentrations of pAAV-DIO-hGAT1^{WT} cre-on virus. *Representative brightfield images of TSA201 cells transfected with Cre-mCherry and transduced with pAAV-DIO-hGAT1^{WT} cre-on. The virus was added in volumes of 10, 20, 40 and 80 µl to the cells. The control shows cre-recombinase-transfected TSA201 cells only, without any virus. Images were taken after a 72h incubation period.*